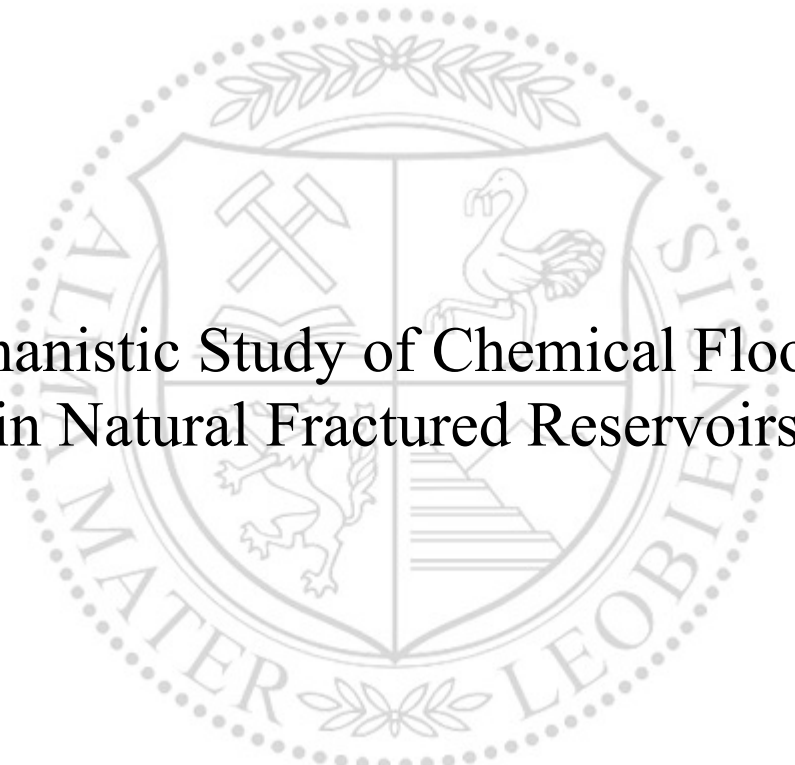Chair of Reservoir Engineering

Master's Thesis

Mechanistic Study of Chemical Flooding in Natural Fractured Reservoirs

Daniel Zettl, BSc

May 2019

Daniel Zettl

Master Thesis 2019 supervised by:
Prof. Riyaz Kharrat

Mechanistic Study of Chemical Flooding in Natural Fractured Reservoirs

dpe DEPARTMENT PETROLEUM ENGINEERING

MONTAN UNIVERSITÄT

EIDESSTATTLICHE ERKLÄRUNG

Ich erkläre an Eides statt, dass ich diese Arbeit selbständig verfasst, andere als die angegebenen Quellen und Hilfsmittel nicht benutzt, und mich auch sonst keiner unerlaubten Hilfsmittel bedient habe.

Ich erkläre, dass ich die Richtlinien des Senats der Montanuniversität Leoben zu "Gute wissenschaftliche Praxis" gelesen, verstanden und befolgt habe.

Weiters erkläre ich, dass die elektronische und gedruckte Version der eingereichten wissenschaftlichen Abschlussarbeit formal und inhaltlich identisch sind.

Datum 28.03.2019

Unterschrift Verfasser/in
Daniel, Zettl
Matrikelnummer: 01235056

I dedicate my thesis to my family who supported me to finish my studies in Leoben. They always believe in me and want the best for me. I also dedicate my thesis to my friends who are my small family in Leoben. We had a lot of fun; there was always someone, who helped me if I had some troubles in my studies or problems with life.

Another fantastic person is my roommate who lived with me for years, which was the best time for me since ever. I hope all the friendships, which were made in Leoben will last forever.

Declaration

I hereby declare that except where specific reference is made to the work of others, the contents of this dissertation are original and have not been published elsewhere. This dissertation is the outcome of my own work using only cited literature.

Erklärung

Hiermit erkläre ich, dass der Inhalt dieser Dissertation, sofern nicht ausdrücklich auf die Arbeit Dritter Bezug genommen wird, ursprünglich ist und nicht an anderer Stelle veröffentlicht wurde. Diese Dissertation ist das Ergebnis meiner eigenen Arbeit mit nur zitierter Literatur.

_____

Name, 27 May 2019

Acknowledgements

Abstract

Natural fractured reservoirs have a large contribution to the world's hydrocarbon reserves. They have usually lower recovery, however a higher residual oil saturation. This is related to different wetting conditions in naturaly fractured reservoirs. Furthermore, natural fractured reservoirs have a lower matrix permeability compared to conventional reservoirs; the porosity for the fracture network is small. By utilizing of the chemical flood (Alkaline – Surfactant – Polymer flooding) in a reservoir with fractured network, it is possible to alter the wettability of the reservoir and decreasing the interfacial tension in the porous medium. Furthermore, it is possible to reduce the mobility ratio, which enhances oil recovery; by utilizing alkaline it is possible to form in-situ surfactants, which are able to reduce the amount of surfactants. Therefore, the residual hydrocarbon saturation will be reduced consequently. Due to the complex reservoir structure and description, chemical flooding operations underestimating the reservoir overall reservoir performance. Due to the natural fracture network, the modelling of chemical floodings will cause issues. It has to be noticed, that the storage occurs only in the pore volume of the matrix, however, the fractures have a significant contribution to the flow through the reservoir and the overall reservoir performance. This master thesis presents a comprehensive study on modeling ASP flooding in naturally fractured reservoirs and mainly addresses capillary forces, gravity, and viscous forces, fracture properties along with fractures using a dual porosity – dual permeability model. By looking into the mechanisms that are behind the oil recovery in different balances of forces, an insight will be given when and why tertiary recovery is working in reservoirs with a fracture network. To some extent, it addresses the effect of capillary and gravity number during the chemical flood acting in the naturally fractured reservoir and the possibility to relate the dimensional numbers with oil recovery rate by using a three-dimensional plot. Related to the benefits of Response Surface Methodology and extensive sensitivity analysis, a Tornado plot should give a broad insight, on how different varying reservoir and constraint parameters are affecting the oil recovery. In addition, the thesis addresses the performance of the oil recovery factor by diversifying fracture spacing, fracture, and matrix permeability as well.

Zusammenfassung

Es wurde festgestellt, dass natürlich frakturiere Lagerstätten einen sehr großen Beitrag zu den weltweiten Reserven liefern. Natürlich frakturierte Lagerstätten haben für gewöhnlich eine niedrige Produktion, aber eine höhere Ölsättigung. Dieses Verhalten kommt von den unterschiedlichen Benetzungsbedingungen innerhalb der Lagerstätte. Zudem haben natürlich frakturierte Lagerstätten, eine geringere Matrixporosität im Vergleich zu konventionellen Lagerstätten; die Porosität der Frakturen ist im Vergleich dazu klein. Durch die Nutzung einer chemischen Flutung (Alkali – Tensid – Polymer Flut) in natürlich frakturierten Lagerstätten, ist es möglich die Benetzung innerhalb der Lagerstätte zu verändern, als auch die Grenzflächenspannung zu reduzieren. Es wird weiters möglich, das Mobilitätsverhältnis zu reduzieren, welches die Produktionsperformance erhöht; durch die Nutzung von Alkali-Flutung ist es möglich, lokale Tenside herzustellen, die den allgemeinen Tensidverbrauch reduziert. Als Folge daraus wird die restliche Ölsättigung konsequent reudziert. Wegen der komplexen Struktur, als auch der Lagerstättenbeschreibung, wird die Performance stets unterschätzt. Bezogen auf die natürlich frakturierten Lagerstätten, kann dieses Verhalten zu Problemen bei der Modellierung führen. Es muss beachtet werden, dass die hauptsächliche Speicherung von Kohlenwasserstoffen im Gestein selbst stattfindet, während die Frakturen einen großen Beitrag zum Fluss durch das Gestein liefern. Diese Masterarbeit befasst sich mit einer umfassenden Untersuchung in der ATP-Flutung von natürlich frakturierten Lagerstätten und bezieht sich dabei auf Kapillarkräften, Gravitäts- und viskosen Kräften, Eigenschaften von Frakturen durch die Benutzung von einem Dual-Porosität – Dual-Permeabilität Modell. Durch Hinterfragen des Mechanismus, der hinter der Gewinnung bei verschiedenen Kräftegleichgewichten steckt, wird ein Einblick in die Funktionsweise der Tertiären Kohlenwasserstoffgewinnung gegeben. Zu einem gewissen Maße beschäftigt sie sich auch mit dem Einfluss von dimensionslosen Kennzahlen wie Kapillaritäts- und Gravitätszahl während einer chemischen Flutung und wie diese dimensionslose Kennzahlen mit dem Ölgewinnungsfaktor in einer dreidimensionalen grafischen Darstellung in Beziehung zueinander gebracht werden können. In Bezug auf die Vorteile der Response Surface Methode und einer Sensitivitätsanalyse, kann ein Tornado Diagramm eine breite Einsicht geben, wie sich die variierenden Lagerstätten und Zwangsbedingungsparameter auf den Ölgewinnungsfaktor auswirken. Außerdem beschäftigt sich diese Masterarbeit mit dem Einfluss von variierenden Frakturendichte, Permeabilität von Frakturen und Matrix auf die Performance des Ölgewinnungsfaktors.

Table of Contents

List of Figures

List of Tables

Nomenclature

A	cross-section	$[m^2]$
c	compressibility	$[1/Pa]$
dp/dx	pressure gradient	$[Pa/m]$
g	gravity constant	$[m/s^2]$
h	height	$[m]$
H	reservoir height	$[m]$
k	permeability	$[mD]$
L_i	block size length	$[m]$
L	reservoir length	$[m]$
M	mobility ratio	$[-]$
N_c	capillary number	$[-]$
p	pressure	$[Pa]$
q	velocity	$[m/s]$
u	Darcy velocity	$[m/s]$
V	volume	$[m^3]$
w	fracture width	$[m]$

Subscripts and Greek Symbols

a	average
b	bulk
cv	capillary to viscous
d	density
e	confining
f	fracture
g	gravity
gv	gravity to viscous
h	healing or height
i	initial or index
m	matrix
o	oil
s	solid
w	water

ρ	density	$[kg/m^3]$
σ'	interfacial tension	$[N/m]$
σ	shape factor	
μ	viscosity	$[Pas]$
ϕ	porosity	$[-]$

Abbreviations

ASP	Alkaline – Surfactant – Polymer
EOR	Enhanced Oil Recovery
DCA	Dual Continuum Approach
DNF	Discrete Fracture Network
DOE	Design of Experiment
DP/DP	Dual Porosity / Dual Permeability
NFR	Natural Fractured Reservoir
RSM	Response Surface Model
PVT	Pressure – Volume – Temperature

Chapter 1

Introduction

1.1 Background and Context

The main goal in this master thesis was to establish the relationship between recovery factor and capillary/gravity forces during a chemical flood in naturally fractured reservoirs. A sensitivity analysis was done in a commercial reservoir simulator to establish a complex relationship in a fractured reservoir by calculating the recovery factor as a function of capillary and gravity number. For the sensitivity analysis, the benefits of Design of Experiments and Response Surface Methodology were used. As a result, it would be able to build a surface model that is a three-dimensional graphical representation of the complex relationship. Due to the results of the RSM, a Tornado plot was generated for each scenario, which showed the various impacts on the oil recovery factor.

1.2 Scope and Objectives

The thesis treats complex behavior during a chemical flood in a natural fractured reservoir. The focus lies on the analysis of the forces acting within the reservoir matrix and fractures during an Alkaline-Surfactant-Polymer flood, which is influencing the recovery factor at the end. One of the objectives is to quantify the recovery factor as a function of capillary/gravity force that was acting during the chemical flood and to show a graphical representation of the complex relationship. This should be done by generating a three-dimensional surface model. Another objective is to show, how the different input parameters are affecting the oil recovery factor by using a Tornado plot. Various sets of matrix and fracture permeability should give an insight into how the oil recovery factor will be affected.

1.3   Achievements

It was possible to show at different reservoir properties, which forces are dominating the recovery factor by using a mathematical approach. The approach in the reservoirs simulator software gives only the numbers of recovery factor and capillary/gravity force. However, a table of numbers at each reservoir property set is confusing. For a better understanding of the complex relationship, it is necessary to represent the numbers as a three-dimensional plot. This would be done by a surface model, which describes the recovery factor as a function of gravity and capillary number in 3D.

1.4   Overview of Dissertation

The beginning of the thesis treats with the important objectives of determining the relevant forces during a chemical flood influencing the recovery factor in naturally fractured reservoirs as well as the essential scope to reach all the given targets successfully. In addition, the literature review represents an overview of the classification and general properties of naturally fractured reservoirs, the rock, and fluid interactions, the reservoir modeling approach and recovery mechanisms within a naturally fractured reservoir. Afterward, a general discussion is held about tertiary recovery and how it will improve the oil recovery in a fractured reservoir. The technical part explains the mechanisms and approaches, which were used to compute the different numbers during a chemical flood in fractured reservoirs. In addition, it includes a representation of the data, the model construction, and information about production and injection constraints. At the end of the reservoir simulations, graphical representations of the results were given such as oil saturation profiles and Tornado plots. A discussion of the results and conclusion including future work will be presented at the end of the thesis.

Chapter 2

Literature Review

2.1   Natural Fractured Reservoirs and Their Properties

2.1.1 Importance and Limitations

Ahmed (2010) stated that more than 50% of reservoirs are naturally fractured reservoirs and have an extensive contribution to the worldwide production of hydrocarbons. These highly heterogeneous formations have a complex fracture network with different spatial distribution and conductivity throughout the geologic formation. Applying a reservoir characterization study on natural fractured reservoirs is a challenging task because they present an extreme property contrast between rock matrix and fractures. It has been stated that almost 60% of the world's proven oil reserves and 40% of the world's hydrocarbon gas reserves are found in carbonate formations (Akbar et al. (2000) and Ahmed (2010)). This indicates that fractured reservoirs are becoming a major issue for the entire world. A significant number of discovered oil and gas fields happen to be fractured and their development constitutes a challenge for the E&P industry. Natural fractured reservoirs (NFR) have been the subject of large-scale studies during the past decades. Common representatives for a fracture system are carbonate and shale reservoirs. However, sandstone formations are able to contain a fracture network as well. Natural fractures exist in practically all reservoirs, dividing the reservoir rock into different segments, called matrix blocks and fractures. In this case, a differentiation between matrix and fracture porosity and permeability is needed. However, in case of no existing fractures or they were isolated or filled with minerals, the reservoir acts as a single continuum with single reservoir porosity. If the matrix blocks have reservoir quality and the fracture network is interconnected, then the reservoir cannot be modeled as a single continuum reservoir anymore and leads to the multiple continua concept. The fundamental issue is finding the right

description of fluid exchange between matrix and fracture blocks. Barenblatt et al. (1960) were one of the first who introduced a mathematical approach to consider the fluid exchange between the matrix block and the fractures. In general, fractures within the reservoir can have a large impact on reservoir performance. Ahmed (2010) stated that, if the reservoir is e.g. a carbonate formation, these fractures create complex paths for fluid movement and influence the reservoir characterization and reservoir performance as well. A significant number of parallel fractures are forming fracture passages where the fractures are closely packed together. As a result, they form a volume that typically is some meters wide, some tens of meters high and many hundred meters long. These fracture corridors act as a highway for fluid flow in the reservoir and the knowledge of their positions within the carbonate formation is important to produce reliable results from reservoir simulation studies. In general, there are several important factors when considering fractures within a reservoir. It is possible that fractures strike and dip in the same direction and their productivity is related to their density, opening, and connectivity. Fractures vary in size, both horizontally and vertically. An example of a carbonate formation is the Selma fractured chalk in Gilberton oil field, located in Alabama. Aguilera (1987) figured out that no matrix porosity was found in the chalk and the fracture porosity was associated with the fault zone. Another example of fractured carbonate reservoirs is the Tamaulipas limestone in Mexico. Producing hydrocarbons from shale reservoirs are common since the early 1900s along the margin of the Appalachian Basin, United States. Generally, a sandstone is ideally composed of quartz grains with a grain size of 62 μm to 2 mm and silica cement, with minimal fragmented particles, which allows sufficient reservoir porosity and permeability for fluid flow. However, unclosed fractures in the sandstone formation can have a significant impact on the reservoir flow and performance. A natural fracture network not only enhances the overall porosity and permeability of the reservoir, but also generates a significant anisotropy, which causes the drainage area around a well to be elliptical. An example of a natural fractured sandstone reservoir is the Altamont trend, Uinta basin of Utah in the United States.

2.1.2 Classification of Naturally Fractured Reservoirs

In general, several classifications exist in the literature. Nelson (1982) proposed a classification of naturally fractured reservoirs, which is based on the percent of total porosity and permeability. The parameters range in percent related to matrix versus percent related to fracture. In reservoirs of type I the fractures control porosity and permeability. Regarding a type II reservoir, the fracture network has a large contribution to the reservoir permeability, while in type III, the fissures were supporting the reservoir permeability. In case of type IV reservoirs, the fractures provide no additional permeability or porosity, however, they can create anisotropic barriers. The classification can be seen in detail in Figure 1.
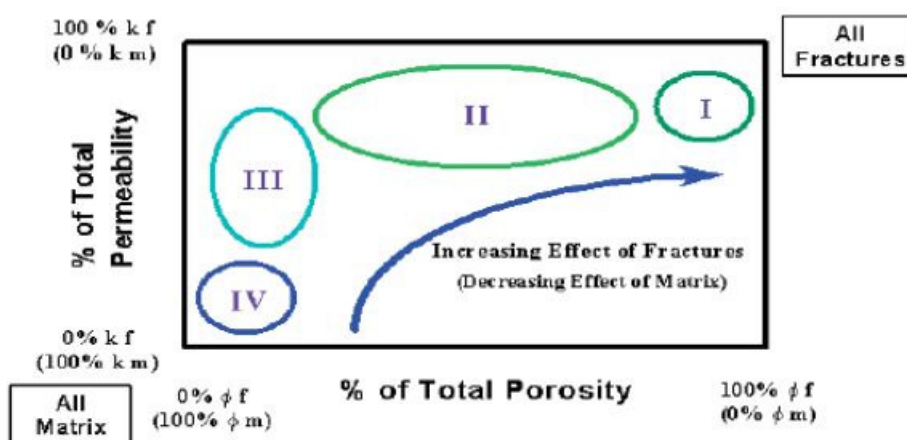
Figure 1 – NFR classification after Nelson (1982)

Aguilera (1998) proposed another classification of naturally fractured reservoirs, visualized in Table 1 depending on porosity and permeability of the matrix and the fractures. Reservoirs of type A have a major proportion of porosity provided by the matrix meaning most of the fluid is stored in the matrix and the fractures provide only a very small storage capacity. In type B reservoirs, almost half of the crude oil storage is in the matrix and in the fracture network. In the case of reservoirs of type C, the hydrocarbon storage is within the fractures. This means the matrix storage capacity has a very low contribution to the total storage of fluid in the reservoir rock.

Table 1 – NFR classification after Aguilera (1998)

Type A	Major proportion of porosity provided by the matrix
Type B	Almost equally proportion of porosity in the factures and the matrix
Type C	Major proportion of porosity provided by the fractures

2.1.3 Fractured Rock Properties

2.1.3.1 Porosity

Porosity can be classified as primary or secondary. Primary porosity is generated during deposition of sediments and can be subdivided into interparticle and intraparticle porosity. Interparticle porosity means there is void space between the grains which can be filled up with fluids. In contrast, intraparticle porosity refers to very small cracks within the grains. Secondary porosity is formed after deposition during diagenetic processes like chemical dissolution and dolomitization. Ahmed (2010) stated that matrix porosity could be both primary and secondary; however, the fracture porosity is always secondary porosity and related to porosity that occurs along with breaks in the sediment or rock body. Fractures enable fluid flow and as a consequence solution of minerals. Regarding the amount of solution, the resulting pores can be classified as molds, solution-enlarged molds or vugs. Vuggy porosity is a non-matrix selective porosity and is caused by several dissolution processes of grains in a rock. If vugs and molds are interconnected with fractures then their individual volume becomes part of the fracture porosity. The fracture network can be observed on cores or on outcrops studies. The fissures can be characterized as open fractures, semi-filled or completely filled fractures. If the fracture is filled with minerals, it does not contribute to the porosity system. The fractures can be horizontal or vertical. The orientation of the fractures is important for their description. How important the fracture porosity is, depends on the type of the natural fractured reservoir. If the fractures have small contribution to storage, however a large contribution to fluid flow, it is not important to know the fracture porosity. In reservoirs where the magnitude of matrix porosity is several orders higher compared to the fracture porosity, early estimation of the fracture porosity is not relevant. If the contribution of the fracture porosity to porosity and permeability is extensive, it is important to have knowledge of the storage volume of the fracture system as early as possible. The knowledge is relevant to evaluate the reservoir and to design a proper

development plan. Related to the large difference of the importance of fracture porosity, it is common to establish the species of the reservoir as soon as possible.

2.1.3.2 Permeability

The permeability is the ability to transmit fluids through the rock body. Similar to the porosity the reservoir can have primary and secondary permeability. The primary permeability is linked to the matrix permeability, which is caused by interconnected pores. The second permeability can be described as fracture permeability or solution vugs permeability. Both permeabilities are important parameters to evaluate the contribution of the fracture permeability to the overall reservoir performance. The fluid flow rate q through fractures can be described by a narrow cleavage and is given by Lamb's law in Equation 1:

$$q = -\left(\frac{W^2}{12}\right)\frac{A}{\mu}\frac{dp}{dx} \qquad \text{Equation 1}$$

Where W is the effective fracture aperture (fracture width), A is the fracture cross section, μ is the fluid viscosity and dp/dx represents the pressure gradient. Darcy's law describes the flow rate as following:

$$q = -k\frac{A}{\mu}\frac{dp}{dx} \qquad \text{Equation 2}$$

Where k represents the permeability. Both equations are valid for laminar fluid flow. A combination of Equation 1 and Equation 2 will give the permeability of a single fracture:

$$k = \frac{W^2}{12} \qquad \text{Equation 3}$$

Aziz and Settari (1985) published an example, with a fracture width of $10^{-5}\,m$ and a permeability of 844 Darcy. The consequence of Equation 1 represents that the flow between two flat plates is proportional to the cube of the fracture aperture W. In fact that the fractures are not as smooth as shown in Figure 2, the relationship could be not true for natural fractures.

Figure 2 – Representative fracture in sandstone after Jones (1975)

In Figure 3, a fractured solid cube is shown and can be calculated as follows:

$$k_{ef} = k_f \frac{W}{a}$$

Equation 4

$$\frac{W}{a} = \phi$$

Equation 5

The fracture porosity is represented in Equation 5. Inserting Equation 5 in Equation 4 results in:

$$k_{ef} = \phi_f k_f$$

Equation 6

As it can be seen, combining Equation 3 and Equation 4 will give the effective permeability k_{ef} and is direct proportional to the cube of the fracture aperture W:

$$k_{ef} \propto W^3$$

Equation 7

In addition, the effective permeability is calculated as followed:

$$k_e = k_{ef} + (1 - \phi_f)k_m \approx k_{ef} + k_m$$

Equation 8

However, the approximation is valid if $\phi \ll 1$.
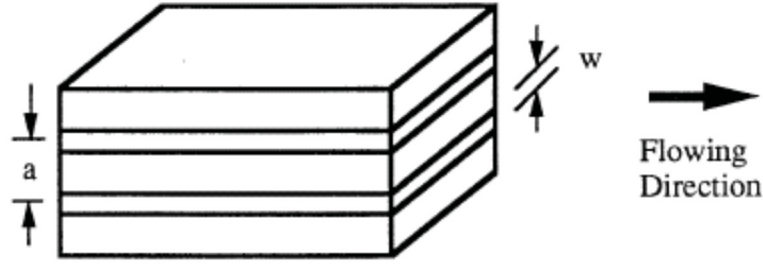
Figure 3 – Fluid flow between parallel fractures after Heinemann and Mittermeir (2014)

2.1.3.3 Compressibility

Confining and pore pressures are determining the stress on the reservoir rock. The confining (or overburden) pressure $\bar{\sigma}$ is caused by the weight of the overlying rock and is partially compensated by the fluid pressures p in the pores. The pressure p_e represents the net confining pressure and is the difference of two pressures (confining pressure minus pore pressure) as it can be seen in Equation 9:

$$p_e = \bar{\sigma} - p \hspace{6cm} \text{Equation 9}$$

A number of research studies indicate that the effect of the varying pore and confining pressure on porosity and permeability is mainly caused by the net confining pressure and is not extremely dependent on the absolute values of either total pore fluid pressure or confining pressure. A typical stress-strain curve manifesting three regions can be seen in Figure 4. The linear relationship of the elastic deformation exists up to stress called yield stress. From this point on the material shows a plastic behavior. If the stress is increased significantly, this will cause a non-linear increase or behavior of strain. If the strain is reduced to a certain amount, the graph does not retrace the original load path of the stress-strain curve. It rather follows an elastic path typical of more consolidated rock. Finally, if there is enough stress applied on the rock, the solid material becomes fully compacted and the stress-strain behavior regains linearity. As an example, the yield point of consolidated sandstones may exceed $1380\ bara$ ($20.000\ psia$), while the yield point for soft chalk can be as low as $60 - 70\ bara$ ($800\ to\ 1.000\ psia$).

In general, the isothermal compressibility factor is defined as the specific volume change caused by the change of pressure:

$$c = -\frac{1}{V}\left(\frac{\partial V}{\partial p}\right)_T \hspace{5cm} \text{Equation 10}$$

The volume V could be related to the bulk volume V_b, the solid volume V_s or the fluid volume V_f. The pore volume of a solid rock matrix and therefore, the porosity has no
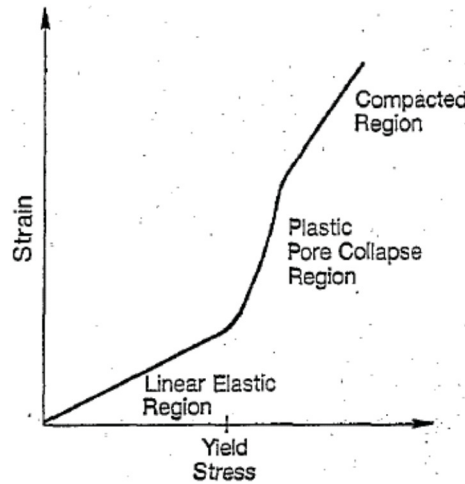
Figure 4 –Rock stress-strain curve after Ruddy et al. (1988)

compressibility. They only change because the solid phase material is compressible. If there is no compaction below the yield point possible, the solid grain volume of a porous rock could be expanded towards the pore volume only. Therefore, it is necessary to define an apparent pore compressibility factor c_ϕ:

$$c_\phi = \frac{1}{\phi}\frac{d\phi}{dp} = \frac{1-\phi}{\phi}c_s \qquad\qquad \text{Equation 11}$$

The c_s represents the compressibility factor of the solid phase. The matrix block will expand towards the fractures if the matrix is tight or porous and surrounded by fractures. As it can be seen in Equation 12, the compressibility of the fracture porosity could be calculated by the compressibility of the matrix bulk volume as followed:

$$c_{\phi f} = \frac{1-\phi_f}{\phi_f}c_b \qquad\qquad \text{Equation 12}$$

If the matrix is tight, the following condition will arise:

$$c_b = c_s \qquad\qquad \text{Equation 13}$$

The matrix porosity compressibility is considerably smaller than the fracture one. In addition, the fracture compressibility cannot be considered as a constant over the entire reservoir pressure decline. Jones (1975) suggested a mathematical expression that would describe the behavior of the fracture compressibility:

$$\frac{\phi_f}{\phi_{fi}} = \frac{\log(p_e/p_h)}{\log(p_{ei}/p_h)} \qquad\qquad \text{Equation 14}$$

The subscript i denotes the value of the variable at the initial condition. In Equation 14 the confining pressure (overburden pressure) is described by p_e and p_h and is related to the

apparent healing pressure. The last one is the pressure, at which the fracture would be closed. Heinemann and Mittermeir (2014) stated that the fracture behavior in limestone, dolomite, and marble is sufficiently similar to be represented by the same expression. All of them having an apparent healing pressure of approximately $40.000\ psia$ ($2700\ bara$). Jones (1975) was able to show that the fracture compressibility in a $20.000\ ft$ deep dense carbonate reservoir is $96.10^{-6}\ psi^{-1}$ at initial pressure and decreases to about $72.10^{-6}\ psi^{-1}$ at depletion. Matrix porosity compressibility factors mainly range between 2.10^{-6} and $15.10^{-6}\ psi^{-1}$.

2.1.4 Rock and Fluid Interaction

2.1.4.1 Wettability

Working in a dual-porosity fractured reservoir, the wettability is one of the most influential factors. Wettability has a significant impact on oil and gas production. It has to be noticed, that the wettability not only determines the initial fluid distribution. The wettability is also important for the flow process, taking place within the rock. It is common, that the wetting phase (e.g. water) tends to occupy the smaller pores of the permeable medium, while the non-wetting phase (e.g. oil) is migrating into the larger pores and fractures. Therefore, wettability has an essential influence on the fracture-matrix interaction and ultimate recovery factor. Ahmed (2010) stated that the wettability of a rock-fluid system is the ability of one fluid in the presence of another one to spread on the surface of the rock. The contact angle θ between liquid-solid interfaces is used to establish the degree of wetting reservoir grain particles by liquids. This angle is always measured through the liquid phase to solid. The concept of wettability can be seen in Figure 5.
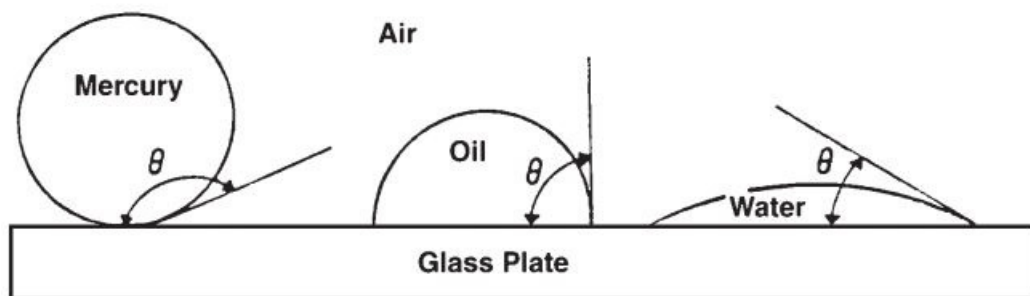
Figure 5 – Illustration of wetting behaviour for various liquids after Ahmed (2010)

Small drops of three different fluids (mercury, oil, water) are placed on a glass plate. In general, it is noted that mercury retains a spherical shape; the oil droplet has an approximated hemispherical shape. However, water tends to spread over the surface of the glass plate. An indication of the wetting characteristics can be done, if one fluid has the tendendy to spread over a solid material surface, in the presence of another fluid. As illustrated in Figure 5, as the contact angle decreases, the wetting behavior of the liquid increases. If the contact angle is zero,

complete wetting condition occurs. Complete non-wetting condition develops if the contact angle is 180°. Ahmed (2010) stated that many intermediate wettability definitions were existing in the reservoir engineering literature. Treiber and Owens (1972) published data, which show that most of the carbonate reservoirs are oil-wet, while sandstone reservoirs can have equal water- or oil-wet conditions. The result of the investigation for reservoir wetting conditions can be seen in Table 2.

Table 2 – Reservoir Wetting Conditions after Treiber and Owens (1972)

Wettability	Contact Angle [°]	Number of Reservoir Investigated		
		Sand	Carbonate	Total
Water wet	0-75	13	2	15
Intermediate wet	75-105	2	1	3
Oil wet	105-180	15	22	37

2.1.4.2 Capillary Pressure

As it is stated in the literature by Heinemann and Mittermeir (2014), the capillary forces in a petroleum reservoir were the result of a combination of different parameters. One important parameter is the surface and interfacial tensions between the rock and fluids, which were stored in the matrix. The pore size and the pore geometry of the reservoir matrix and the wetting conditions within the system are influencing the capillary pressure as well. They said, if the surface interface between two immiscible fluids (water and oil) is curved, it tends to contract into the smallest possible area per unit volume, which is related to the theory of minimum surface energy. The discussion about the curvature is only true if the fluid combination is oil and water, (gas and water) or oil and gas related to reservoir fluids. Therefore a pressure discontinuity will exist between two immiscible contacting fluids. This important effect will depend on the curvature of the fluid interface. This pressure difference is called capillary pressure and is referred by p_c. In addition, if one fluid is displaced by another one (water is displacing oil in a waterflood process) in the pores of a porous medium, the process is highly depending on the capillary forces. Heinemann and Mittermeir (2014) discussed the problem if the fracture capillary pressure has an influence on the fluid exchange between the matrix and a single fracture. In multiphase flow, the matrix and fracture network behave fundamental different. They said it is commonly accepted that capillary pressure in fractures is zero or negligible for the fractures and these are assumed physically correct fracture properties. There is no doubt, that capillary pressure can be present in the fracture network. The rise of a meniscus

in a capillary tube is similar to the effect between two plates where the void space between the plates represents the fracture. They presented an example of a capillary pressure calculation in fractures by using the equation of Laplace. If the fissure has a width of $d = 0.1\ mm$, a capillary pressure of not more than $0.003\ bara$ will be calculated. Discontinuities in the rock, characterized as fissures, have greater apertures and smaller capillary pressures. Which results in no practical application. Another important point is that the capillary pressure in fractures cannot be measured on a natural rock sample. For measurements, the fractures cannot be extracted from cores and broken samples cannot be restored. Heinemann and Mittermeir (2014) said it has to be discussed seriously, if the fracture capillary pressure has an significant impact on the fluid exchange between matrix and fracture network. Normally, commercial simulation software offers possibilities to implement a capillary pressure for the fracture network too. However, they stated it is not recommended to apply it. The fracture capillary pressure should be considered as zero.

2.1.5 Characterization Methods of Fractures

2.1.5.1 Direct Sources of Information

Heinemann and Mittermeir (2014) said that a direct source of information includes outcrops analysis, core and image logs. Performing an extensive core analysis, it will provide remarkable information for the fracture characterization process. Cores can be used to analyze the relationship between single fractures and the reservoir rock material. Muskat (1946) stated that cores and outcrops provide extensive material for routine and advanced reservoir engineering analysis (e.g. PVT analysis) as well as broad information about the geo-mechanical features of the fractures. An important example would be the timing of the fracture development relative to the reservoir diagenesis. Other important parameters for the development of the fracture model are single- and multi-fracture parameters. From thin sections of the core, various single-fracture parameters can be obtained such as fracture width, size, and orientation. It would be vital to do fracture description for the whole core before the core is sliced. A combination of fracture morphology (open, filled, partially open fractures) and fracture size and orientation gives relevant information. The fracture orientation gives an explanation of the fracture's induced anisotropy. It is important to measure the fracture aperture and height because it makes it possible to compute the fracture density, fracture porosity, and some more relevant fracture properties. Regarding multi-fracture parameter, the areal fracture density A_{fd} can be inferred from thin-section core analysis and was stated by Heinemann and Mittermeir (2014):

$$A_{fd} = \frac{number\ of\ fractures * length\ in\ thin\ section}{area\ of\ the\ thin\ section} \qquad \text{Equation 15}$$

In contrast, the linear fracture density is inferred from the intersection of fractures along a vertical line. The major problem in core analysis is that the most cores are drilled from vertical wells. Due to vertical drilling, they intersect vertical and horizontal fractures. Cores from several outcrop studies can provide the understanding, how fractures were formed during history related to stratigraphy and lithology. The observation is made either on the reservoir rock formation or on a rock chosen based on similarity to the reservoir in stratigraphic setting, lithology, rock properties, age, structure, etc. The main issue with outcrop analysis is that the same stress history cannot be assumed at the surface and a depth of thousands of meters subsurface. If rock material uplifted to the surface, the overburden pressure is removed. In addition, erosional processes take place and the tectonic stress is reduced. The temperature is reduced due to surface temperatures exposition and the pore fluids pressure will change significantly. Another source for gaining information about the fracture network is image logs. These methods are used in the industry for fracture observations: acoustic imaging logs and resistivity based image logs. Image logs based on resistivity measurement measure the resistivity of minerals and produces a high-resolution resistivity image of the borehole wall. Several arrays of electrodes are dragged along the borehole wall to generate resistivity images. In contrast, acoustic imaging logs utilize an acoustic pulse for borehole wall imaging. Heinemann and Mittermeir (2014) stated that the wall of the borehole is scanned with a specific scanning tool. The scanning procedure of the borehole works with a narrow pulse acoustic beam and from rotating several transducers. During the approach, the logging tool is pulled out of the hole continuously. For the measurement, the amplitude and travel time reflected from the wellbore wall are recorded with the same transducer that generates the acoustic beam. For the orientation of the images, a magnetic sensor is used. From the image logs the location, size, and orientation of the fractures intersecting the wellbore can be observed, providing a 360° view of the borehole. There are however some issues with these logging tools. One of them is that they are not applicable to oil-based mud. In contrast to water-based mud, there is a potential to differentiate open fractures filled with mud filtrate from water-filled fractures if resistivity tools are used. Resistivity tools can be used to observe fracture aperture and in addition calculating fracture porosity.

2.1.5.2 Indirect Source of Information

Heinemann and Mittermeir (2014) said that core and image log analysis as it was discussed before, provides the most accurate data about the presence of fractures and their geometry. However, such core and image analysis might not indicate the real effect of fractures on the fluid flow if these measurement tools are used alone. If the observed information from core and image measurement tools are combined with other sources, the knowledge about the fracture

network increases significantly. The indirect methods for information gathering come from drilling and production history, log analysis and well tests. These methods can provide information about the transmissivity (connectivity of fracture system and conductivity), the fracture storativity (fracture size, aperture, and intensity), the anisotropy (stress field) or the areal and vertical reservoir heterogeneity. If the circulation is lost during drilling, it could be an indication for fractures, underground caverns or induced fractures during the drilling process. Applying tracer tests to the reservoir provides an inexpensive, direct indication of fracture connection and directional tendencies. A tracer fluid is injected into a well and the surrounding wells are monitored for the presence of the tracer. A limitation of tracer tests might be the long response time and well interference tendencies. Different well logging tools like porosity logs can be used to recognize open fractures. However, there is no further discussion included in this thesis. Well test analysis gives valuable information about the fracture system as well. The pressure analysis can be used to evaluate the fracture, matrix and combined permeability and porosity. In a fractured reservoir, the same parameters as for well tests interpretation in conventional reservoirs can be observed, such as kh. It should be noted that well test analysis as a single indicator was not recommended for a naturally fractured reservoir since the dual porosity response in the analysis is very limited and could give misleading interpretations. It is common that many NFRs do not show dual porosity behavior in well test analysis. It should be considered that the transition between the fracture and entire system flow is often reached very rapidly so that it is completely masked by wellbore storage effects. Heinemann and Mittermeir (2014) stated that the application of interference tests in naturally fractured reservoirs can be used as a direct indication of fracture connectivity. This gives a measure of the permeability anisotropy, which is an important parameter because systems have a strongly preferred orientation.

2.1.6 Reservoir Modelling Approach

One approach to model fractures within a reservoir is the method of "Discrete Fracture Network (DNF)". In this model, planes or disks represent the fissures and fractures. For many years, it was common practice to not include it in geologic realism. Heinemann and Mittermeir (2014) stated that the reason for this is, that the planes or disks (representing the fractures) were randomly distributed in the reservoir model. For the reservoir modelling the fracture density (function of reservoir thickness), the reservoir lithology and other geologic drivers should be not ignored because these parameters will affect the reservoir performance at the end. Since DNF models were introduced to implement fracture distribution within a natural fractured reservoir model, there was a need for constraining the realization for geologic input. Some efforts have been made to control the fracture generation with some indicator. However, only one geologic driver was considered, the others were ignored and more importantly, the complex

interaction of the drivers was not taken into account. The concept of conditioned DFN was introduced by Ouenes and Hartley (2000). They represented a way for integrating all the important geologic drivers (fracture permeability, fracture density and more) in a continuous fissure model. At the end, it was possible to use this application and to constrain the DFN. Zellou et al. (2003) were able to publish a recent field example related to conditioned DFN. Another approach is the Dual Continuum Approach (DCA). As mentioned before, it can be distinguished between primary and secondary porosity, the same distinction can also be made for permeability. Warren and Root (1963) stated that in general, both classes of porosity are present in the reservoir rock and the internal void volume of the rock has a significant intermediate character. This explanation refers to an independent system of secondary porosity and is superimposed on the primary porosity. The idealization and representation of an intermediate porous medium is a combination of discrete volumetric elements with primary porosity representing the matrix porosity matrix blocks, which are coupled anisotropic by secondary volumetric elements representing the fracture porosity with void space between the matrix blocks as shown in Figure 6.
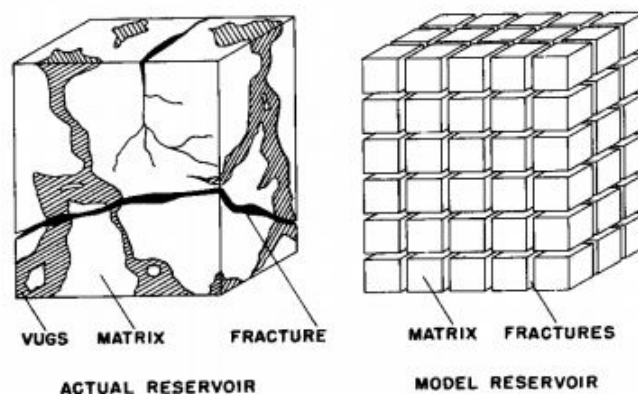
Figure 6 – Idealization of the heterogeneous medium after Warren and Root (1963)

The approach of Warren and Root (1963) includes only the dual porosity – single permeability behavior, where the fluid is stored within matrix and fractures, but the flow takes place only in the fractures. Improvements on the before mentioned approach led to the introduction of dual porosity – dual permeability behavior which was commonly used by Gilman and Kazemi (1988), Festoy and van Golf-Racht (1989), Uleberg and Kleppe (1996) and others. The updated approach allowed modeling the fluid flow within the fractures and the matrix as well. In addition, fluid flow equations have to be established for the matrix block, the fractures, and transfer functions as well as for the interaction between matrix block and surrounding fractures. A simple representation of the dual porosity – dual permeability relationship can be seen in

Figure 7. The dual porosity model allows the fluid storage in the matrix block and the fracture network, however as mentioned before the fluid flow takes only place within the fractures. In the case of the dual permeability model, the fluid storage is comparable to the dual porosity model. Though the fluid flow is now allowed within the matrix block and the fracture network as it can be seen from Figure 7 where all blocks are connected.
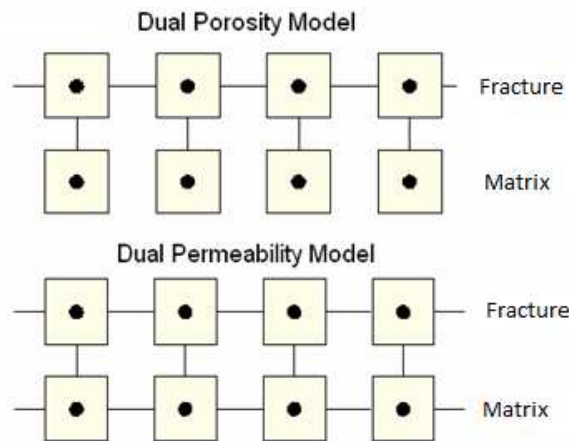
Figure 7 – Model Concepts (CMG Ltd, IMEX User Guide, Version 2014)

2.2   General Recovery Mechanisms in NFR's

As for non-fractured, single porosity systems, the same processes are active and important for fractured reservoirs. These processes include rock compaction, fluid expansion, solution gas drive, gravity drainage, viscous displacement, capillary imbibition, and diffusion. It should be considered, that the main amount of the hydrocarbon is stored in the high porosity/low permeability matrix system. While the well depletes mainly from the high permeable fissures (benefit of increased production performance). Hence, the two systems have a varying degree of importance for the physical mechanisms.

2.2.1   Fluid Expansion and Solution Gas Drive

Heinemann and Mittermeir (2014) stated that, because of hydrocarbon production, the pressure drops in the fracture network rapidly, fluid starts to expand depending on fluid compressibility and expel from the matrix to equilibrate the matrix pressure with fracture pressure. In addition, the compressibility of rock has an important contribution to production performance. The pore compressibility for fracture and matrix are different in cases. If the reservoir system is below bubble point pressure, the solution-gas liberates and starts to expand. Muskat (1981) and Pirson (1958) established approaches for the calculation of the efficiency of matrix recovery under solution gas displacement. Muskat (1981) and Pirson (1958) did a lot of work on material balance calculation and were able to show that the reservoir performance in case of solution gas drive can be written in a differential form of the material balance.

2.2.2 Gravity Drainage

If the fluid contents of the matrix block and the fracture network are not the same (e.g. the fracture is completely filled with water or gas and the matrix is filled with oil), a significant discrepancy in the hydrostatic head exists. This is due to gravitational force exists between the matrix block and fracture system (density difference between the fluids). Due to this additional potential difference, the water or gas is forced from the fracture into the matrix while the oil is expelled of the matrix.

2.2.2.1 Gravity Drainage Assuming Homogeneous Vertical Saturation

For explanation, a matrix block surrounded by fractures is considered. The matrix block is saturated by oil and the fracture is filled by either water or gas as it can be seen in Figure 8. If no capillary forces were acting on the system, there would be no difference in phase pressures: $p = p_o = p_g = p_w$. In the middle of the matrix block (blue dashed line), the pressure is equal and referred to the pseudo-steady state. Regarding a transient process like well testing, the pressure could be various at this point but then it will be equalized rapidly. Due to the different hydrostatical gradients, a pressure difference is created above and below the midpoint as it is shown in Figure 8 which was published by Heinemann and Mittermeir (2014). If the fracture is completely filled by water, the water will imbibe the matrix at the bottom of the block and the oil will be expelled at the top of the matrix block. In case the e of gas-filled fracture the gas enters at the upper half of the matrix and the oil will be expelled at the lower one. The average hydrostatic pressure difference is calculated as the following:

$$P_{hwof} = \frac{1}{2} h_m (\rho_w - \rho_o) g \hspace{3cm} \text{Equation 16}$$

In the previous calculation h_m represents the vertical extension of the matrix block.
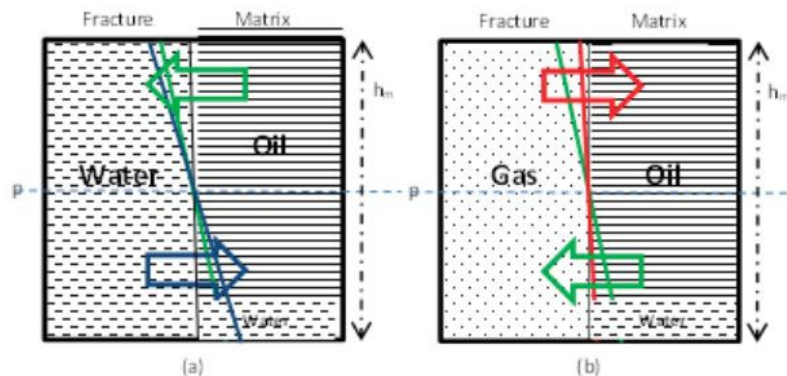
Figure 8 – Vertical pressure distribution in matrix and in fracture a) filled with water b) filled with gas after Heinemann and Mittermeir (2014)

2.2.2.2 Gravity Drainage Assuming Phase Segregation

Regarding phase segregation, three different cases are considered: two-phase water-oil case, two-phase gas-oil case, and three-phase case. For the two-phase water-oil case Figure 9 illustrates an idealized matrix block surrounded by fractures and both the matrix and surrounding fractures contain oil and water and was originally published by Heinemann and Mittermeir (2014). If perfect phase separation is assumed both in the matrix block and fracture system, the hydrostatic pressure difference can be calculated as follows:

$$P_{hwof} = h_{wf}(\rho_w - \rho_o)g \qquad \text{Equation 17}$$

$$P_{hwom} = h_{wm}(\rho_w - \rho_o)g \qquad \text{Equation 18}$$
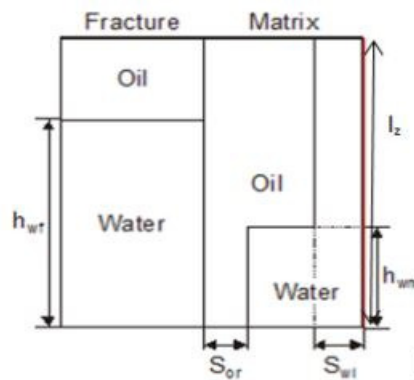
Figure 9 – Two-phase segregation of oil-water filled matrix
and fractures after Heinemann and Mittermeir (2014)
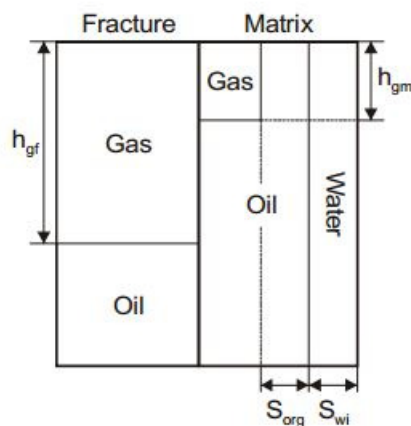
Figure 10 – Two-phase segregation of gas-oil filled matrix and
fractures after Heinemann and Mittermeir (2014)

For the two-phase gas-oil case, Figure 10 illustrates an idealized matrix block surrounded by fractures and both the matrix and corresponding fractures contain oil and gas. Similarly, the hydrostatic pressure difference for the two-phase gas-oil case can be calculated in the same way as the water-oil case. For the three-phase case with segregated fluid saturation, the model can be handled as a combination of the before mentioned two-phase cases. Figure 11 illustrates an example of a three-phase case. It should be noted that the saturation distribution in the matrix could be naturally more complicated. Different displacement mechanisms could act one after the other. As an example, a solution gas drive can be followed by water displacement and afterward a gas displacement could occur. Quandalle and Sabathier (1989) published an alternative approach for three-phase segregation.
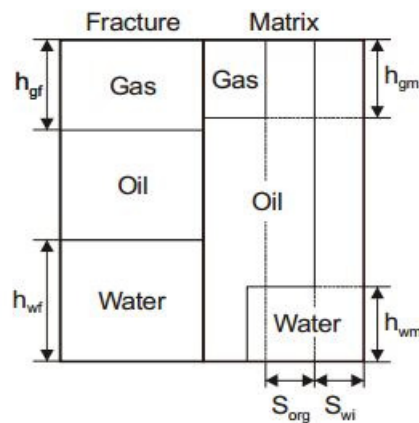
Figure 11 – Three-phase segregation of multi phase filled matrix and fractures after Heinemann and Mittermeir (2014)

2.2.3 Viscous Displacement Process

The viscous displacement process of fluids takes place when a pressure difference enforces the fluids to flow. Regarding a dual porosity system, the flow of the fluids towards the production wells will cause a significant pressure gradient within the fracture network compared to the matrix system. It should be noticed that the fracture has a very high effective permeability and hence the pressure gradient inside the fractures will be small. Regarding to this information, the viscous forces acting between fracture and matrix can be neglected. Otherwise, if the fracture has a moderate permeability magnitude, viscous forces will affect the fluid flow between matrix block and fractures substantively. Figure 12 illustrates a representative matrix block with known dimensions that is surrounded by fractures, where the fluid flow takes place from the left to the right side and was published by Heinemann and Mittermeir (2014). They said that the inlet fracture pressure (p_1) is higher compared to the outlet (p_2) and the average fracture

pressure (p_f). In the case of a water flow in the fractures, a greater pressure gradient is required to expel oil from the matrix.
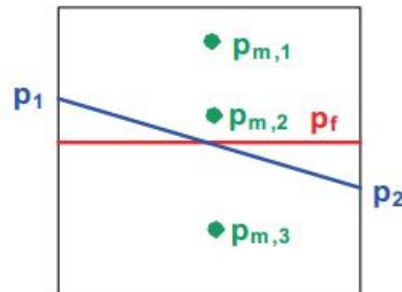
Figure 12 – Viscous displacement model after
Heinemann and Mittermeir (2014)

2.2.4 Capillary Imbibition

For demonstration, a piece of porous rock, called matrix with surrounded fractures can be imagined. The matrix block is assumed to be water-wet and given oil saturation. The water starts to invade the fractures, driven by capillary forces the water invades the matrix and displaces the oil in a countercurrent way. This means the water imbibes the matrix block from the same side where the oil is expelled. The configuration of the fracture network can be two or three-dimensional and has a significant impact on oil displacement. For simplification, it can be assumed to be one-dimensional. Figure 13 shows a core that is sealed on all sides except the bottom surface. The core is oil-saturated and at connate water saturation. As shown in Figure 13, the core is contacted with the wetting phase. Because of capillary forces, the wetting phase (water phase) tends to imbibe at the bottom side and thus displace the non-wetting phase (oil phase) in countercurrent flow. For the calculation of the displacement process, the following assumptions have to be made:

1. The rock is homogeneous
2. The displacement process is one-dimensional
3. Both phases are incompressible and immiscible
4. Multiphase Darcy's equation is valid for the process

Heinemann and Mittermeir (2014) established an approach for the calculation of the capillary imbibition displacement process based on Figure 13. Blair (1960) presented a numerical solution for the model defined in the before mentioned figure.
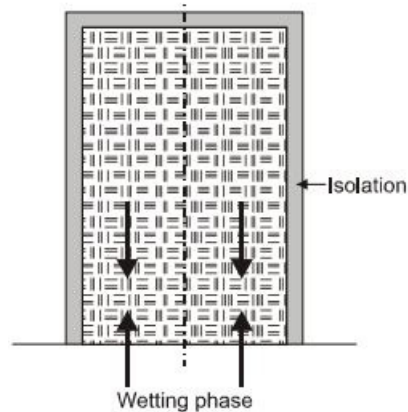
Figure 13 – Visualization of the countercurrent imbibition after Blair (1960)

2.2.5 Molecular Diffusion

In contrast to no fractured reservoirs, the molecular diffusion in naturally fracture reservoirs may be very important, because the dispersive flux through the fracture network rapidly increases the contact area for diffusion. Analogical, Fick's law of molecular diffusion potential may dominate viscous displacement forces when the fracture spacing is very small and hydrocarbon or inert gases are injected into the reservoir. Heinemann and Mittermeir (2014) stated that the following approach is used to calculate the diffusion process between the matrix blocks and the fracture planes. It should be mentioned the procedure is not utilized for grid blocks within the same grid system. In addition, the method can be utilized to calculate gas-gas and gas-liquid diffusion rates. Da Silva and Belery (1989 - 1989) published the before mentioned approach. Injecting hydrocarbon gas at pressures below the bubble point pressure might lead to two-phase diffusion. For instance, if the injected gas is dispersed throughout the fractures might contact large areas with two-phase saturated matrix blocks. As a result, of concentration differences, the injected gas tends to diffuse through both hydrocarbon phases, which concurrently causes counterflow to the fracture system. It should be noticed that the gas-gas diffusion is almost ten times faster than the gas-liquid diffusion. The mixing mechanism observed during multicomponent fluid displacement in porous rock media is typical of the convection-diffusion type. An important statement is that convection results from the reservoir heterogeneity inducing several significant local bulk velocity differentials, while diffusion refers to the random motion of molecules within the phase. Both mechanisms combined causes dispersion, which is defined as a mechanism, which will tend to abrogate any spatial concentration differences and would another important recovery mechansim. In general, the

dispersive flux of a particular fluid component depends on the concentration gradients for each involved component.

2.2.6 Transfer Functions

Barenblatt et al. (1960) originally formulated the transfer function as an integrated part in the so-called dual continuum concept. These transfer functions are used to describe the flow from the matrix to the fractures. Barenblatt et al. (1960) assumed that fluid flow takes place within the fracture network only. The matrix only acts as a container for the reservoir fluids. With the initially proposed mathematically equations, it was possible to describe the fluid flow from the matrix block into the fractures under certain assumptions. All of the before mentioned flow processes can occur one followed by the other one within a natural fractured reservoir. In addition, several reflections have to be made for a sufficient transfer function description.

2.3   Tertiary Recovery in Naturally Fractured Reservoirs

Application of successive waterflooding in natural fractured reservoirs includes water-wet matrix conditions and enough amount of water to inject it into the reservoir. Tang and Firoozabadi (2000) were able to show that in some experiments the water flood performance in the water-wet and intermediate-wet fractured carbonate reservoirs may be nearly independent of the wettability state. In addition, Babadagli (2000) proposed that capillary imbibition significantly improves oil recovery under favorable water-wet conditions. Bourbiaux and Kalaydjian (1990) stated that an important type of capillary imbibition is the spontaneous imbibition of the wetting phase, which involves the concurrent and concurrent flow of fluids in different directions in different proportions and was depending on the ratio of gravity/capillary forces and on the existing conditions at the matrix boundaries as well. Controlling variables for the capillary imbibition are matrix permeability, size and shape, wetting conditions, reservoir heterogeneity, and boundary conditions. Furthermore, several properties of the imbibing water, viscosities of the phases and interfacial tension (IFT) affect the capillary imbibition recovery rate. In some cases, unfavorable conditions may exist in NFRs, which includes heavy oil, oil-wet reservoirs, large matrix sizes, low matrix permeability, and high IFT. All these features could interfere with the normal dynamics of oil displacement within the reservoir. Babadagli (2000) was able to show two methods to deal with high existing mobility contrast, including the injection of surfactant solution to reduce IFT, and/or adding a polymer solution to the injected water. Therefore, chemical flooding in natural fractured reservoirs is generally concerned with the influence of surfactant/alkali and polymer injection on the dynamics of oil displacement. Regarding to tertiary recovery, there are other approaches available like steam

injection, gas injection and foam injection. However, only the chemical tertiary recovery methods like surfactant, alkaline and polymer flooding operations will be discussed in this work.

2.3.1 Surfactant Flooding

The oil production from water flood in mixed-wet or oil-wet natural fractured reservoirs are normally unsatisfactory because the water flows in the permeable highways (fractures) with minor spontaneous imbibition of water into the matrix block. Therefore, extensive laboratory and simulations work has been performed to study the application of surfactant flooding in fractured reservoirs to improve oil recovery. Generally, surfactants are organic compounds that are composed of a hydrocarbon tail (hydrophobic group) and a polar hydrophilic group ("head") and therefore surfactants are soluble in both organic solvents and water. Sheng (2011) was able to show that surfactants adsorb on or concentrate at rock surfaces or fluid/fluid interfaces to alter the surface properties significantly. At any point, where the porous rock is contacted by surfactants the wetting conditions are altered and as a result, the capillary pressure will be changed, there is a positive effect for relative permeabilities and the residual oil saturations are changed as well. Fadili et al. (2009) stated that the purpose of applying a surfactant flood in the fractured reservoir is to reduce the IFT between oil and water and to change matrix wettability from oil or intermediate-wet to more water-wet. The main mechanism of the chemical flooding is the reduction of residual oil saturation, which is closely related to the capillary number. Based on the concept of capillary number, the decrease in IFT corresponds to the increase of the capillary number and leads to the decrease of residual oil saturation. Sheng (2011) was able to show that if residual saturation starts to decrease at the critical capillary number and continues to decrease until the maximum capillary number is reached. The concept of capillary number is given in Equation 19 where v represents the velocity, μ is fluid viscosity and σ' represents the interfacial tension:

$$N_c = \frac{v\mu}{\sigma'}$$
Equation 19

2.3.2 Alkaline Flooding

Alkaline flooding is an enhanced oil recovery technique utilizing alkaline chemicals like sodium hydroxide, sodium orthosilicate or sodium carbonate and injecting them during polymer flooding or water flooding operations. The main functions of alkaline additives are to advance crude oil emulsification, increase ionic strength while at the same time IFT is reduced, and regulate phase behavior. Utilization of alkaline additives also helps to reduce the adsorption of anionic-chemical additives by increasing the negative-charge density of mineral rocks while making the rock more water-wet. Alkaline flooding acts in-situ forming the surfactant inside of

the reservoir. Manrique et al. (2007) established that is possible to utilize alkaline additives in carbonate reservoirs in case of Alkaline-Surfactant-Polymer (ASP) operations, however, it is generally not recommended in carbonate reservoirs because of the abundance of calcium. A mixture of alkaline chemical and the calcium ions could produce hydroxide precipitation that may damage the formation. Therefore, it is usually recommended only for sandstone reservoirs.

2.3.3 Polymer Flooding

The utilization of a polymer flood has been the most widely used Enhanced Oil Recovery (EOR) method in different sandstone and carbonate reservoirs, to control the mobility of the water, which enhances the reservoir performance. In a significant number of the polymer cases, water-soluble polyacrylamides are used. Biopolymers (polysaccharides and cellulose polymers) to a lesser degree can also be applied for mobility control. Regarding carbonate reservoirs, most of the reported polymer flooding operations used polyacrylamides and were developed in the early stages of water flooding as part of the mobility control strategy. As a result, the sweep efficiency is improved and the final oil recovery of water flood projects is increased. The main function of a polymer operation is to increase the viscosity of the injection phase while decreasing the effective relative permeability. Thereby, the mobility ratio decreases and a higher displacement and sweep efficiency can be achieved. In addition, using a polymer flood can help to plug flow highways like fractures. Due to the high permeability of fractures and an extensive fracture network within the reservoir, an early breakthrough of flooding operations could occur. To resolve this issue, polymer floods have been used for plugging the fractures due to increasing fluid viscosity. As a result, the mobility ratio is increased. It is now possible to get access to the matrix block where the oil saturation is higher compared to the before water flooded fractures. In combining surfactants and alkaline flooding operations, the IFT and therefore capillary pressure can be reduced. Water is now able to imbibe into the matrix block and expel the oil. In the end, areal and vertical sweep efficiency can be increased significantly.

Chapter 3

Technical Chapters

3.1　Technical Paper Review

Several technical papers from different sources were reviewed to find the optimal model for the base case simulation. The main sources for the review were from Cheng et al. (2018), Abbasi Asl et al. (2010), Mohammed and Hossain (2016). The source from Cheng et al. (2018) represents an extensive study of surfactant imbibition mechanisms in fractured reservoirs. However, there is no sufficient database in the technical work included to remodel their presented reservoir model. The source of Abbasi Asl et al. (2010) deals with the chemical transport in naturally fractured reservoirs and provides a sufficient database. However, the data for the reservoir model, reservoir properties, saturation profile, and well constraints is better prepared in the technical work published by Mohammed and Hossain (2016). This work represents the base case scenario for the simulation work in this master thesis.

3.2　Methodology

3.2.1　Model Parameters & Preparation

This section describes how the reservoir model is constructed based on the data published by Mohammed and Hossain (2016). The description of the reservoir parameters, properties of the NFR and the fluids in the system (chemicals and hydrocarbon) were implemented into the commercial reservoir simulators STARS 2018.10 and CMOST 2018.10. Table 3 through Table 7 represents the reservoir properties and PVT data. The reservoir data, matrix properties, fracture properties, fluid properties, well constraints, and saturation values are originally used from the technical paper. The PVT data was given by Bakhsi et al. (2017).

Table 3 – Reservoir Data

Reservoir Data		
Grid Block Size	30 x 30 x 10	ft^3
Number of Grid Blocks	30 x 30 x 4	
Flooding Pattern	Inverse 5 – Spot	
Injector – Producer Distance	636.4	ft
Producer – Producer Distance	900	ft
Reservoir Depth	5000	ft
Reservoir Pressure (@ 5010 ft.)	4000	psi
Reservoir Thickness	20	ft

Table 4 – Matrix Properties

Matrix Properties		
Horizontal Permeability	1	mD
Vertical Permeability	1	mD
Initial Oil Saturation	0.75	
Matrix Porosity	0.2	
Connate Water Saturation	0.25	

Table 5 – Fracture Properties

Fracture Properties		
Fracture Horizontal Permeability	1000	mD
Fracture Vertical Permeability	500	mD
Fracture Initial Oil Saturation	0.99	
Fracture Porosity	0.01	
Fracture Opening	10	ft

Table 6 – Fluid Properties

Fluid Properties	Oil	Water	Polymer	Surfactant	Alkaline
Phase	Oleic	Aqueous	Aqueous	Aqueous	Aqueous
Mass Density [lb/ft^3]	53.6	62.366	62.366	62.366	62.366
Viscosity [cP]	2.01	0.6	70	0.6	0.6

Table 7 – PVT Data

PVT Data		
Bubble Point Pressure	950	$psig$
Oil compressibility (above BP) Oil compressibility (below BP)	0.0000109 0.000375	$1/psi$
Reservoir Temperature	201	$°F$
Gas Gravity (Air = 1)	1.67	

The surfactant used in the flooding operation in the related technical paper presentation from Mohammed and Hossain (2016) was Sodium Dodecyl Sulfate (SDS), the Alkaline was Sodium carbonate (NaCO3) and the polymer was Hydrolyzed Polyacrylamide (HPAM). The properties of these fluids have been obtained from laboratory measurements and were fed to the simulator. In the absence of the possibility to repeat own laboratory measurements, the properties for the ASP flood (interfacial tension) are used from the technical paper presented by Mohammed and Hossain (2016). The concentration for the polymer slug is $0.15\ wt\%$, for the alkaline and surfactant slug, $2\ wt\%$ and $2.5\ wt\%$ is used. These values are recommendations from related papers and literature dealing with chemical flooding in natural fractured reservoirs and conventional reservoirs like Mohammed and Hossain (2016) and others. The half-life time of the polymers is 1040 days, which is the default value from the simulator. Limestone was chosen as a reservoir rock. The saturation profile for an oil-wet reservoir, which is given by Delshad et al. (2009) was used in the simulation and can be seen in Figure 14. For the fracture system, a straight-line relative permeability and zero capillary pressure were assumed as it was discussed by Heinemann and Mittermeir (2014)
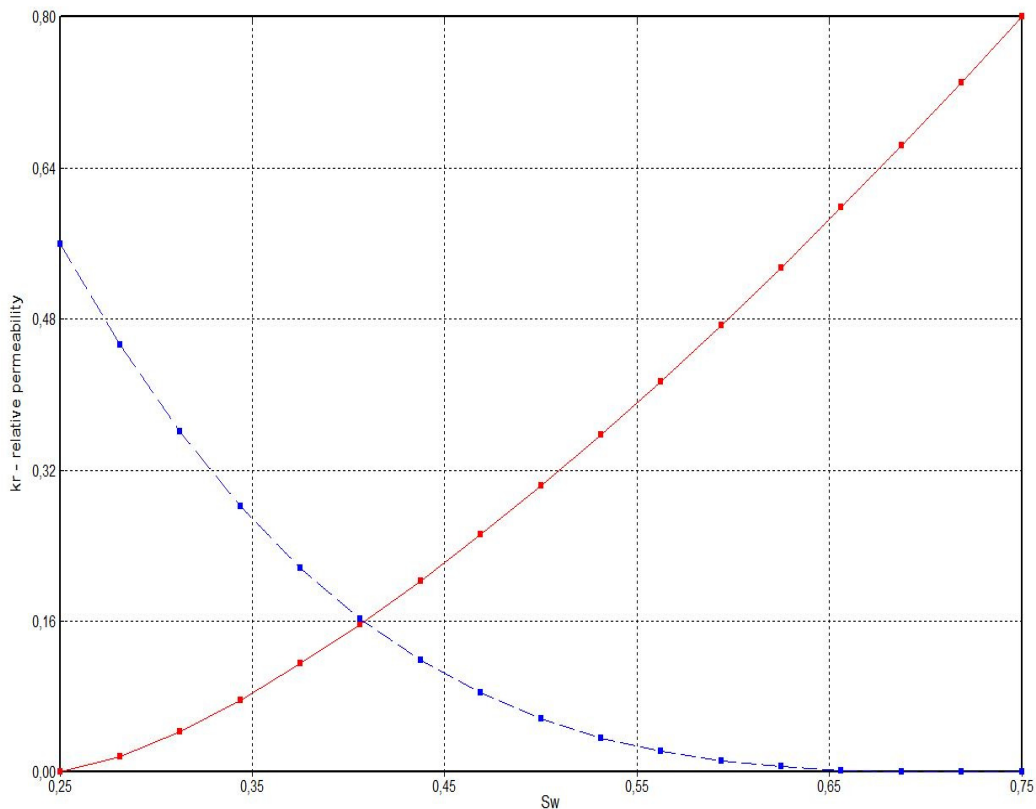
Figure 14 – Saturation Profile

3.2.2 Model Construction

A 30 x 30 x 4 Cartesian grid model has been constructed representing an inverse 5-spot injection pattern with two layers (top layer in blue and bottom layer in red). Where 1800 grid blocks representing the matrix system and 1800 grid blocks are for the fracture network. The grid blocks of the fracture network are overlaying the grid blocks of the matrix system for each layer. The distance between the producers (in each corner of the model) is 900 ft and the distance between injector (in the middle of the reservoir model) and producers is $636.4ft$. The geometry of the constructed reservoir model can be seen in Figure 15.
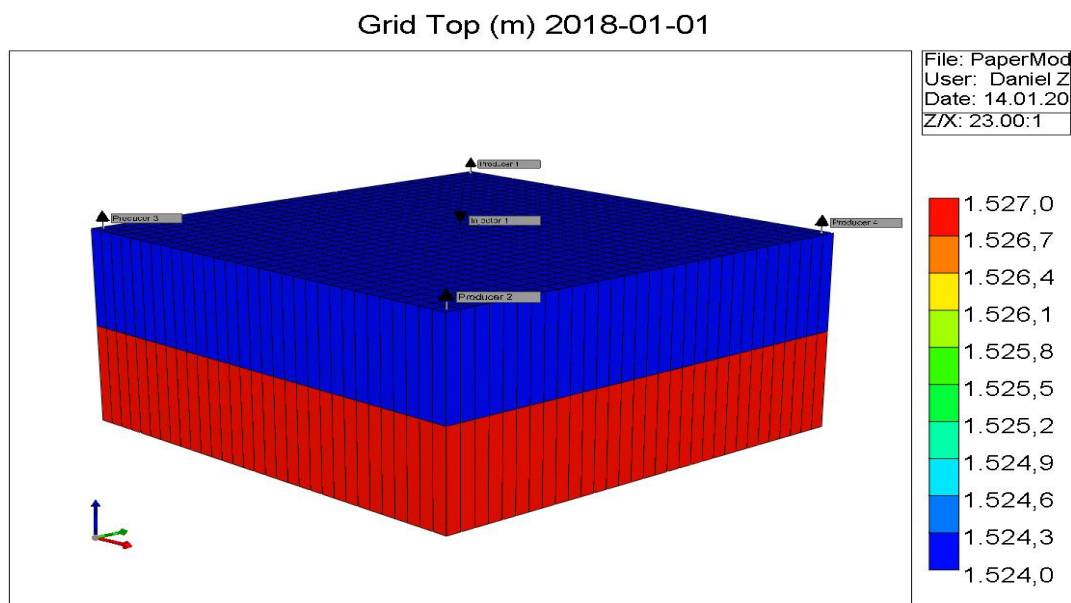
Figure 15 – 3D representation of the reservoir model

3.2.3 Dual Porosity – Dual Permeability Model

The modeled reservoir is constructed in a carbonate reservoir and the fractures are distributed through the whole reservoir. The naturally fractured reservoir is characterized by low flow from the matrix to fracture, but a high flow from the fracture system. Whereas the matrix system acts as a storage medium for reservoir fluids and the fracture system acts as a flow path for the reservoir fluids. To implement the flow characteristics of a fractured reservoir the Dual Porosity / Dual Permeability (DP/DP) model was used. The utilization of the DP/DP model will add a matrix-matrix flow term to the matrix mass balance and the total energy balance equations used in the only dual porosity model. Where this added term is considered zero in the DP model. For the description of the transmissibility function in the fracture-matrix fluid flow, the Gilman and Kazemi shape factor σ was used in the model. The same shape factor relationship was used by Mohammed and Hossain (2016) The following equation describes the shape factor:

$$\sigma = 4 \sum_i \frac{1}{L_i^2}$$
<div align="right">Equation 20</div>

Where L_i is the block size in x, y, and z-direction.

3.2.4 Injection/Production wells

The reservoir model consists of one injection well (in the middle of the model) and four producers (in each corner of the model). A representation of the model and the data for the well constraints can be seen in Table 3 through Table 8. All the wells have the same well diameter of 12 in and the perforations were made at a depth of 5010 ft. The injection periods and sequences for the chemicals were based on the published pilot test and the literature from Saad et al. (1989) and Mohammed and Hossain (2016). The sequences for the base case and the simulations are as follows:

- Water Injection period for 1 Year
- Alkaline-Surfactant sequence for 2 Years
- Alkaline-Surfactant-Polymer sequence for 2 Years
- Low Polymer concentration sequence for 1 Year
- Water Injection period until finishing simulation end

The simulation ran for 25 years, begins on January 1, 2018, and will end on January 1, 2043.

Table 8 – Production / Injection Well Data

Production / Injection Well Data		
Perforation Depth	5010	ft
Well Diameter	12	in
Bottom Hole Pressure for Production Well	1000	psi
Rate Constraint for Injection Well	629	bbl/day
Rate Constraint for Production Well	314	bbl/day

3.2.5 Methods Theory of DOE and RSM

After the setup of the base case for water injection and chemical injection (ASP flood), the sensitivity analysis model has to be created, utilizing the idea of Design of Experiment (DOE) and Response Surface Model (RSM). Heeremans et al. (2006) said that many applications of Experimental Design have been reported in the literature in many areas of petroleum engineering including sensitivity analysis, upscaling, performance prediction, uncertainty modeling, and optimization. Examples of the broad area of applications are water flooding, estimating parameters and assessing uncertainty and to quantify such uncertainty in production forecasts for a population of deep-water channelized sandstone reservoir. In addition, Heeremans et al. (2006) said that a large number of numerical simulations is required to analyze the sensitivity of production with respect to many influencing factors like geology, fluid and engineering parameters in a reservoir model. Implementing all these simulations in a reservoir simulator is time-consuming and expensive. Hence, the need for an approach, which can reduce this high amount of simulation runs to a reasonable number with adequate accuracy, is vital. Especially, when many parameters are analyzed in a sensitivity study. Therefore, the application of DOE and RSM deliver tools to select efficiently a reasonable number of runs and give maximum information from the design space. Based on significant statistical principles, the influence on the resulting performance by varying parameters can be identified. The objective of the DOE approach is to achieve the most reliable results with optimal utilization of time and money. The major and important principle behind Design of Experiment is that it changes a various number of parameters systematically and at the same time within a limited number of experiments (depending on the discrete level) to give an overall view of the analyzed process. Heeremans et al. (2006) presented how the DOE approach works extensively in their technical paper. After completing the process of the Design of Experiments, the Response Surface Model (RSM) approach can be utilized to fit the simulation or experimental results to a model during sensitivity analysis. The method allows visualizing the effect of two of the parameters on the observation parameter(objective function), where the model gets fitted by a polynomial function (proxy model) that considers linear, second order and interaction terms (cross terms) if using a quadratic model for RSM, which can be seen in Equation 21:

$$y = a_0 + \sum_{j=1}^{k} a_j x_j + \sum_{j=1}^{k} a_{jj} x_j^2 + \sum_{i<1}^{k} \sum_{j=2}^{k} a_{ij} x_i x_j \qquad\qquad \text{Equation 21}$$

The variable a represents the coefficients of the model, x_j is the linear term, x_j^2 is the quadratic term and $x_i x_j$ represents the cross term of the model. The Design of Experiments approach is already implemented in the reservoir simulator CMOST, where it is possible to include a various number of parameters affecting the simulation output. For the response surface models, the simulation results from CMOST are implemented into the MATLAB software and a regression tool is utilized to generate a surface model based on a polynomial, where the oil recovery factor is a function of capillary and gravity number.

3.2.6 Influencing and Resulting Parameters

The first step of investigating the performance of water injection and chemical fluid injection in naturally fractured reservoirs is looking at sensitivity issues of these processes and how are they influencing the oil recovery factor. Several parameters were varied such as matrix permeability, fracture spacing, fracture permeability, injection rate, and matrix porosity. The ranges that are used in this experiment are provided in Table 9 and representing the influencing parameters. Two dimensionless numbers are derived for certain reservoir operating conditions to get a feeling on how all these parameters influencing the recovery. These numbers represent different physical forces within the reservoir and describe the relative magnitudes of these forces:

$$N_{vc,m} = N_{vc} * R_t^2 \qquad\qquad\qquad \text{Equation 22}$$

$$N_{vc} = \frac{v * \mu}{\sigma} \qquad\qquad\qquad \text{Equation 23}$$

Equation 23 describes the viscous over capillary forces ratio in the matrix, where v represents the Darcy velocity in the matrix network, μ is the viscosity of the oil and σ is the interfacial tension and R_t^2 represents the scaling group. The equation for the conventional capillary number is implemented in the CMG software using an average velocity from each neighboring matrix block related to the work of Foulser and Goodyear (1989). This velocity represents the Darcy velocity for the calculation of the capillary number. Referring to the work of Heeremans et al. (2006) and Dengen Zhou, F. J. Fayers, F. M. Orr Jr. (1993), they established a capillary number with only the vertical velocity component of capillary pressure. For simplification, the general derivation for the capillary number was used.

$$N_{gv,f} = \frac{\Delta\rho g k_f L}{q_f \mu_o H} \qquad\qquad\qquad \text{Equation 24}$$

Equation 24 describes the gravity forces over viscous forces in the fractures after Dengen Zhou, F. J. Fayers, F. M. Orr Jr. (1993), where $\Delta\rho$ is the density difference between injection fluid

and producing fluid, g is the gravity constant, k_f is the fracture permeability in a vertical direction, and q_f is total Darcy flow velocity in the fracture and is calculated with the same principle as it was done for the capillary number. The variable μ_o represents the oil viscosity. Furthermore, the flow velocities in matrix and fracture network and other related properties for calculation of dimensionless numbers were used from the last time step between injector and producer 1 (User block address: 9,10,2). This means the dimensionless variables represents the flooding behavior at this reservoir block. The scaling group R_t^2 is already implemented in Equation 23.

$$R_t^2 = \left(\frac{L}{H}\right)^2 * \left(\frac{k_{av}}{k_{ah}}\right)$$

Equation 25

The R_t^2 represents the scaling group. R_t^2 is also called the effective shape factor, which is the shape factor (L/H) weighted with the permeability anisotropy. The effective shape factor represents the relative flow capacities of the medium in each direction. The idea behind the effective shape factor is to cover the characteristics of the reservoir within the dimensionless number. Otherwise, the capillary and gravity number represents only the microscopic behavior of the medium. The procedure of scaling dimensionless numbers is based on the work of Shook et al. (1992). After performing the DOE within the software automatically, the simulation output (oil recovery factor, modified capillary, and gravity number) were used for the 3D plotting process.

Table 9 – Coded Parameters for Sensitivity Analysis

Relative Change	Units	Low	Base	High
Fracture Spacing in X-Y-Z Direction	ft	0.984	3.2	20
Horizontal Fracture Permeability	mD	500	1000	1500
Vertical Fracture Permeability	mD	100	500	1000
Matrix Permeability in X-Y-Z Direction	mD	0.1	1	20
Matrix Porosity	–	0.01	0.2	0.4
Injection Rate	bbl/day	314.5	629	943.5

Chapter 4

Results and Discussion

4.1 Results Section

4.1.1 Grid Sensitivity

As can be seen from Figure 16, a sensitivity analysis on the grid size was done to evaluate if there are discrepancies. In addition to the base case (30x30), grid models of significant bigger and smaller grid block sizes (20x20 and 40x40) were built to figure out if there were reasonable numerical errors in calculating the oil recovery regarding the grid size.
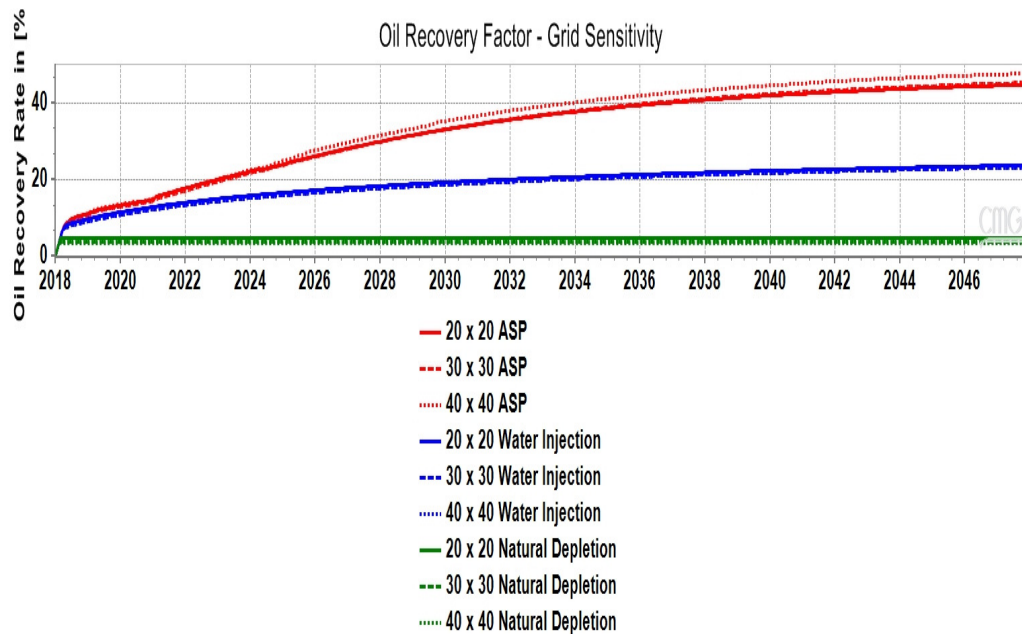
Figure 16 – Oil Recovery regarding to Grid Sensitivity

4.1.2 Depletion Scenarios and Saturation Profiles

A comparison is done for different depletion scenarios using the base case reservoir model. Figure 17 represents the oil recovery from ASP compared with water injection and natural depletion.
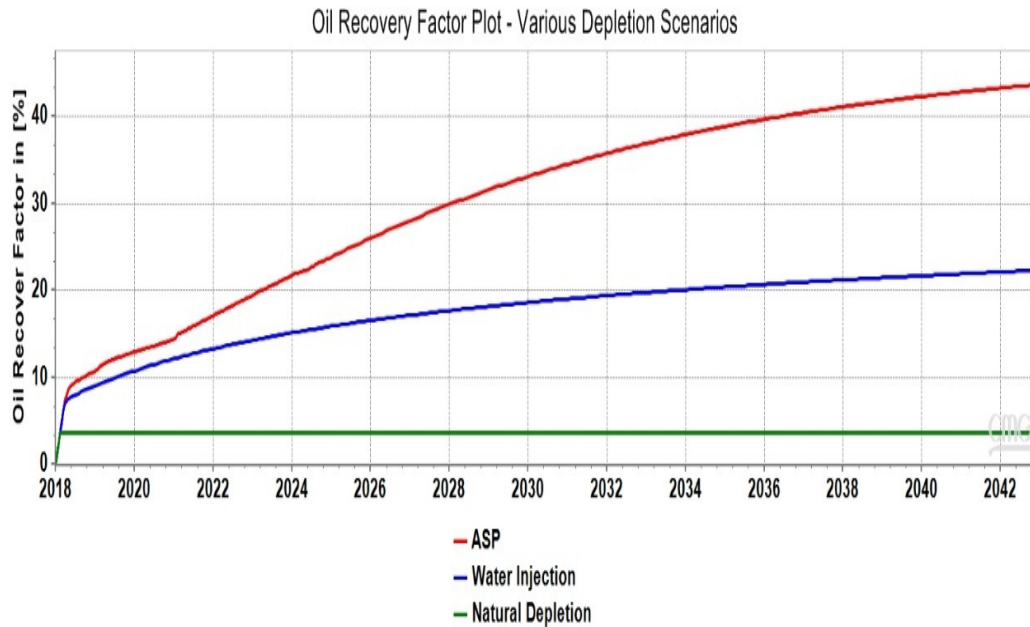
Figure 17 – Oil Recovery Factor for various Depletion Scenarios

Figure 18 and Figure 19 represents the oil saturation of water injection and ASP flood in the base case model. Each saturation profile represents the cross-section of the reservoir, where the injector is positioned in the middle.
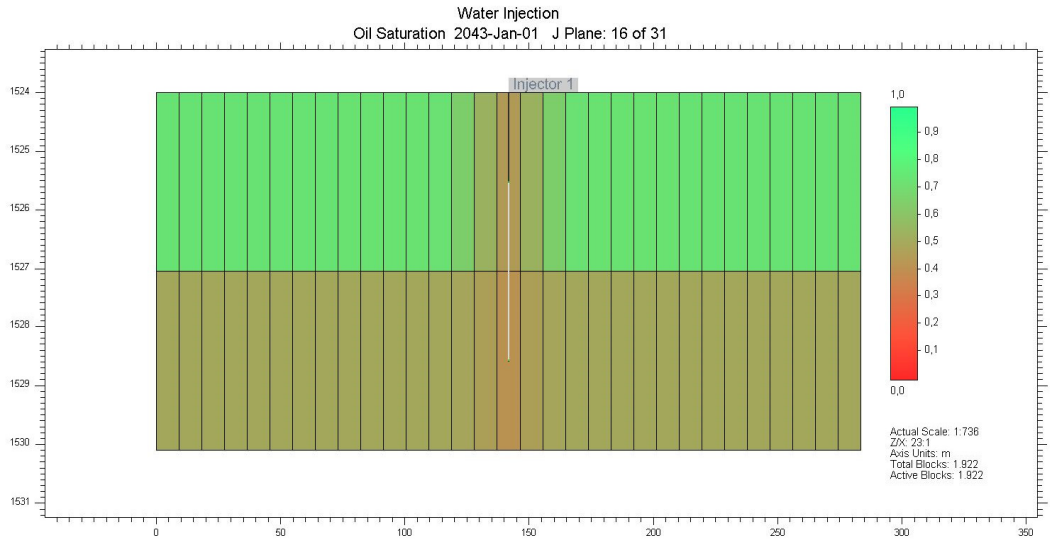
Figure 18 – Oil saturation profile in the matrix of the base case model after water injection at the last time step
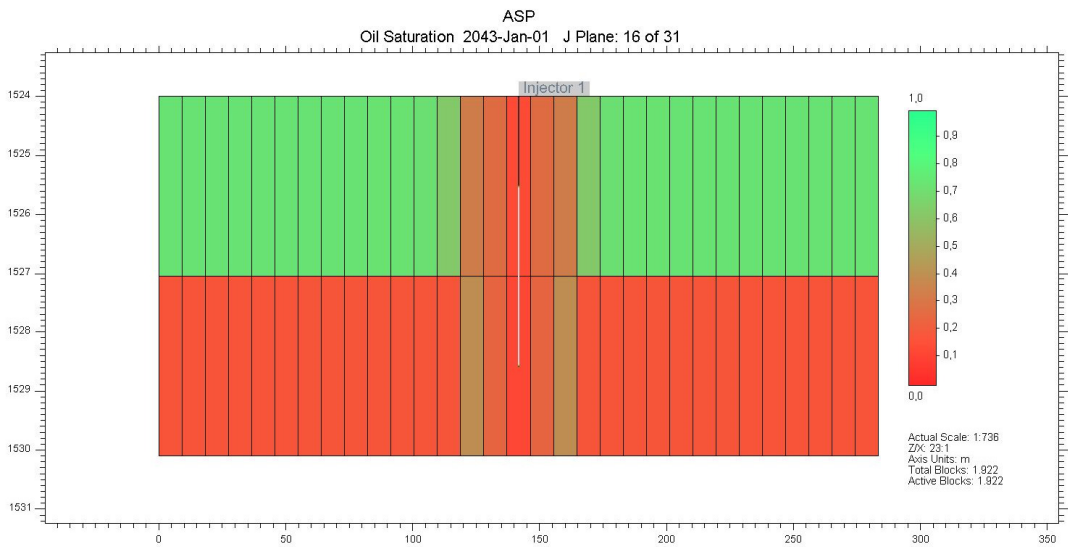
Figure 19 – Oil saturation profile in the matrix of the base case model after ASP flood at the last time step

4.1.3 Matrix and Fracture Permeability Contrast

Figure 20 and Figure 21 represents the difference in oil recovery between homogeneous and naturally fractured reservoir, and the effect of different matrix and fracture permeability on the oil recovery rate.
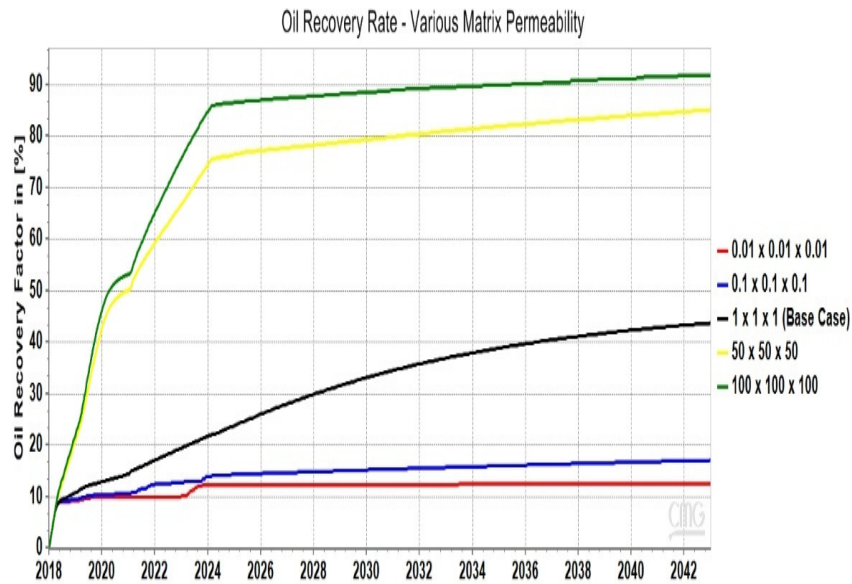
Figure 20 – Effect of different matrix permeability on oil recovery rate
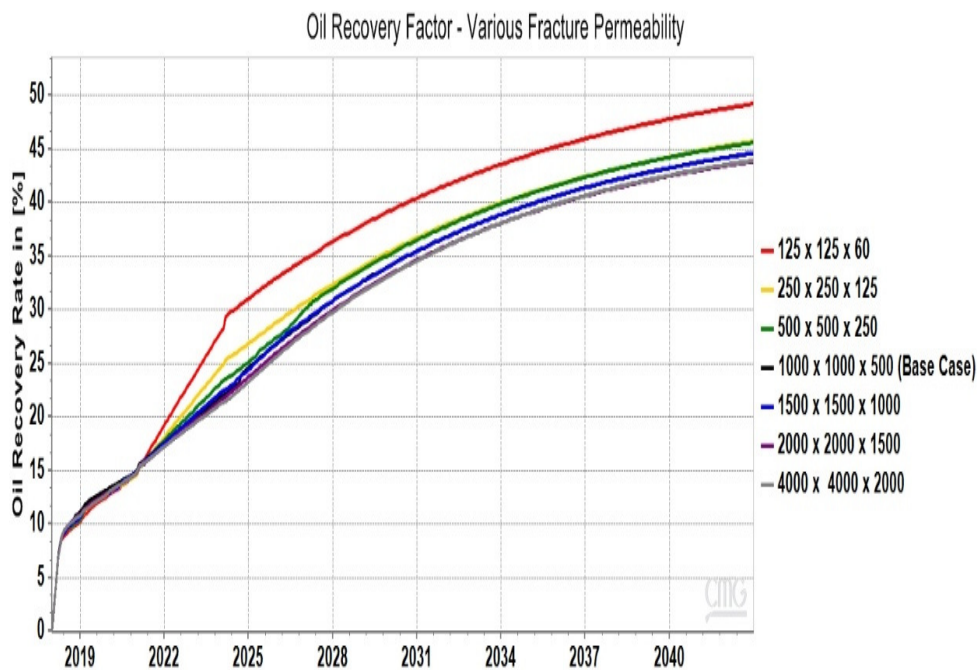
Figure 21 – Effect of different fracture permeability on oil recovery rate

4.1.4 Results from the Response Surface Model

Simulation results from the sensitivity analysis in the CMOST software from CMG for each case should give the recovery factor, capillary number and gravity number. The dimensionless numbers were calculated for a specific matrix block between injector and producer 1 at the last time step (User Block Address 9, 10, 2). After performing the sensitivity analysis, these numbers were fed to the MATLAB software to perform a data analysis, which gave a general polynomial for the oil recovery factor as a function of capillary/gravity number and related coefficients of the polynomial. As a result, the polynomials would be plotted in 3D by using related commands in MATLAB. The code to generate the plots of the surface models can be found in Appendix A. In addition, a top view of a combination of the response surfaces and the 3D representation was shown in Figure 22 and Figure 23. The recovery factor after water injection and ASP as a function of viscous to capillary and gravity to viscous forces can be determined easily from the plots. Table 10 and Table 11 give representative values from the simulation. The discussion of all results will be done in the next section.

Table 10 – Results from Sensitivity Analysis for Water flooding

N_{vc}	N_{gv}	Oil Recovery Factor in [%]	
4.32E-10	37.67	6.22	MIN
1.52E-05	41.37	38.35	AVERAGE
1.97E-05	40.00	42.98	MAX

Table 11 – Results from Sensitivity Analysis for ASP

N_{vc}	N_{gv}	Oil Recovery Factor in [%]	
1.81E-04	48.30	44.18	MIN
5.63E-03	42.49	61.09	AVERAGE
3.73E-03	38.24	88.30	MAX
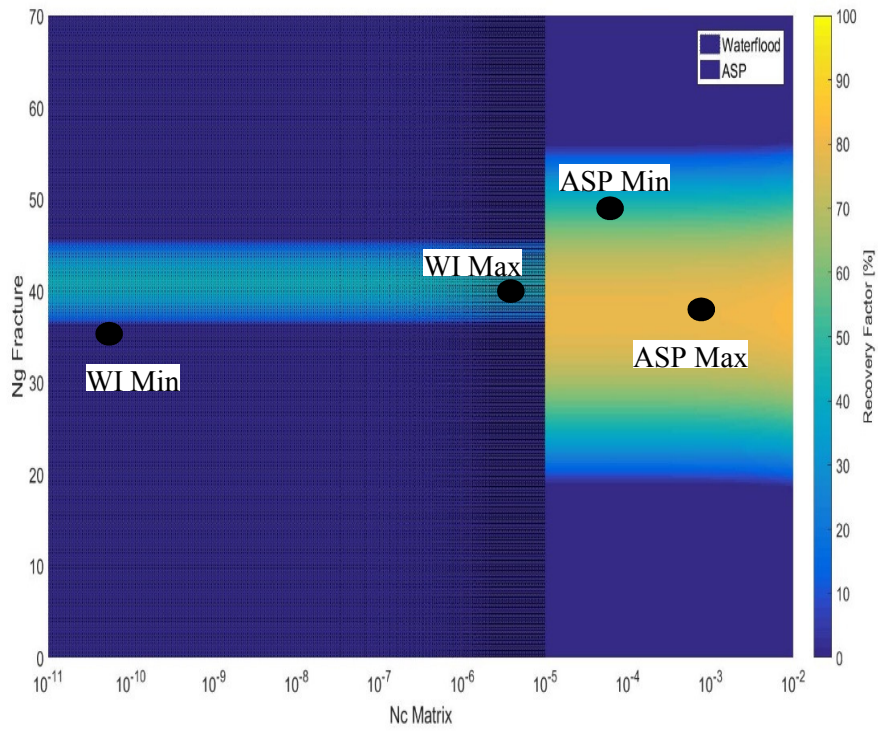
Figure 22 – Top view of the surface models (Water Injection and ASP)
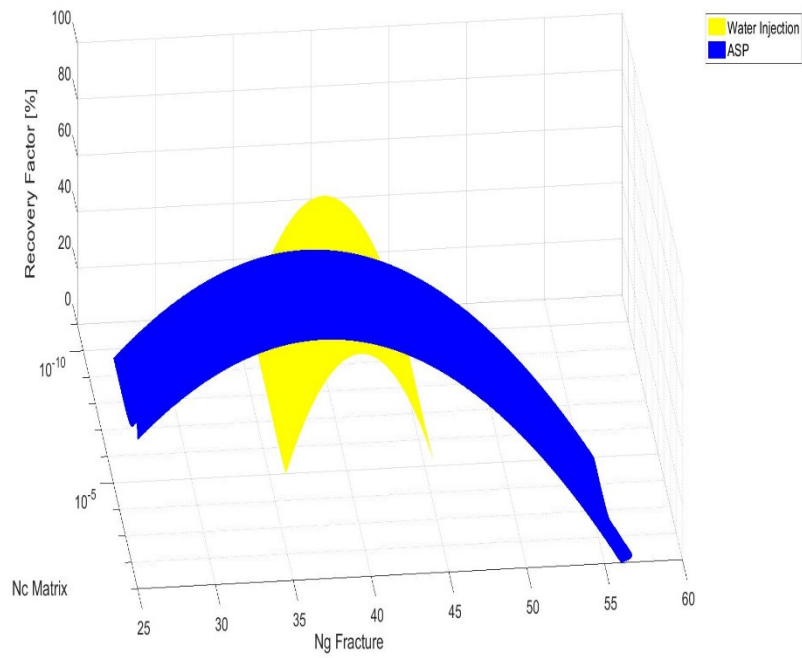
Figure 23 – 3D plot of the surface models

4.1.5 Results of the effect of different parameters (Tornado plots)

The Tornado plots of the different scenarios on the performance of the water and ASP are shown in Figure 24 and Figure 25. The minimum and maximum effect based on the linear term and cross term, for the two floodings, can be observed.

Figure 24 – Tornado plot shows the influences of each term on the recovery of Water Injection
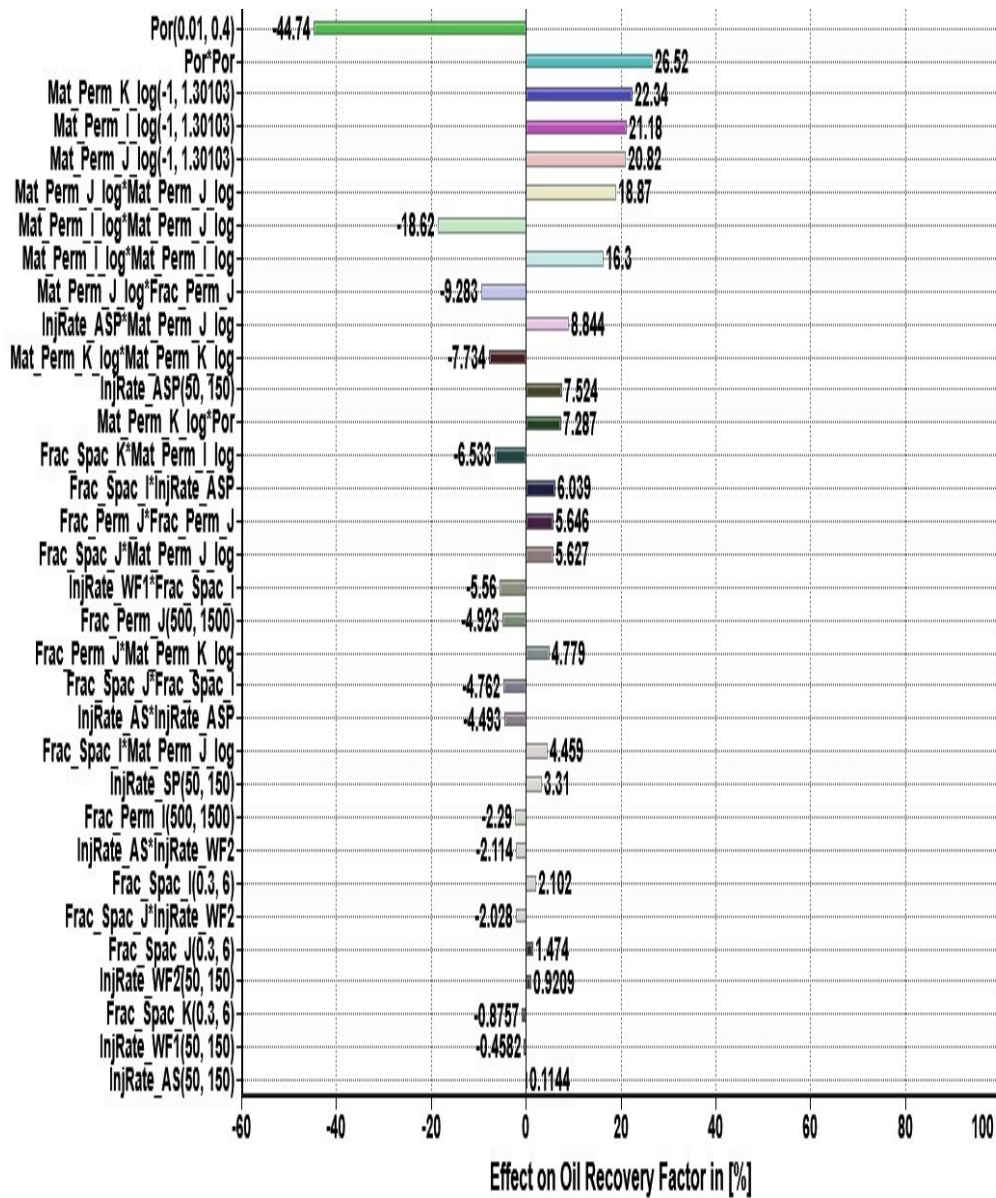
Figure 25 – Tornado plot shows the influence of each term on the recovery of ASP

4.2   Discussion Section

Several simulations have been run to perform a sensitivity analysis for water injection and chemical flooding. The principles of RSM and Experimental Design were used to generate response surfaces. After 25 years of water injection and chemical flooding, the recovery factor as a function of capillary and gravity number could be determined relatively easily with the surface model plot. However, the chosen dimensionless numbers gave not the expected relationship with the oil recovery rate, which means the surface planes gave not representative and correct results.

4.2.1 Grid Sensitivity

In Figure 16, the discrepancy for the oil recovery is very small for the grid models in the water injection case. In comparison to the ASP flood, the 40x40 model slightly performed better as the fine grid model with an error of about 1.5%. However, this error would be acceptable because the base case model did not show a deviated trend in the water injection case.

4.2.2 Depletion Scenarios and Saturation Profile

Regarding the used reservoir properties in the synthetic base case model, the oil recovery had a significant increase for the ASP flood compared to the water injection (an increase of about 20%) as it can be seen in Figure 17. It was assumed, the reservoir is oil wet. Regarding the wetting condition, the water flood is not possible to sweep a significant amount of the matrix. This is related to the capillary imbibition curve of oil-wet reservoirs and the capillary pressure discrepancy. In the absence of significant natural mechanisms, the oil recovery for natural depletion was very low. As can be seen from Figure 17, the ASP flood should be favored because of a better sweep and displacement efficiency within the reservoir compared to the water flood.

In Figure 18 and Figure 19, the oil saturation profile of the base case (NFR) for the matrix system from water injection and ASP flood around the injector (in the middle of the reservoir) can be seen. The residual oil saturation in the ASP flood case is significantly lower compared to inject only water into the reservoir (about 30% of oil saturation difference regarding to the color code) and results from the advantages of using surfactant and alkaline, which mobilize the residual oil in the pores and changing the wettability from oil wet to more water wet. However, in both depletion scenarios, the sweep efficiency in the upper layer was not sufficient. Due to high permeable fractures and increasing fracture density, the displacing fluid was not able to sweep the entire upper layer of the reservoir model and flowed instead to the subjacent layer. In general, related to gravity the displacing fluid will flow in the vertical fractures anyway. This can be seen in the results of the gravity number, where the gravity forces

dominating over viscous forces within the vertical fractures. However, the higher the fracture density and fracture permeability, the lower the possibility that the displacing fluid will penetrate a significant amount of the matrix in the upper layer. To overcome the problem of worse sweep efficiency in the upper layer, the injection rate could be increased significantly, which allows a deeper penetration of the displacing fluid. However, it has to be analyzed technical and economical, how the oil recovery factor will change regarding the increase of the injection rate. Drilling new injection wells could overcome the problem as well; again, the costs for drilling new wells have to be justified by a significant increase in oil recovery to make the project economical.

4.2.3 Matrix and Fracture Permeability Contrast

Figure 20 represents the variation of the matrix permeability within a naturally fractured reservoir. It can be seen, that if matrix permeability increases to a certain point, it will have a positive effect on the oil recovery related to a better displacing fluid transport through the matrix. In Figure 21, the oil recovery factor for different sets of fracture permeabilities can be seen. It is obvious, that if the fracture permeability is increasing, oil recovery will decrease, because of an early breakthrough. The higher the fracture permeability, the higher the possibility, that fluid transport mainly occurs within the fractures. This means a significant amount of the reservoir will be not contacted by the displacing fluid. The several simulations of the permeability contrast and fracture spacing indicate that ASP performance is affected to some extent. This effect is related to the increase in the residence time of the injected chemicals and the faster imbibition between matrix blocks and fractures.

4.2.4 Results from the Response Surface Models

As can be seen from Table 12 and Table 13, the general trend of increasing oil recovery by increasing capillary number was matched. For the minimum case in water flooding, the oil recovery was very small. The capillary number was small as well, which indicates that the capillary force was significantly higher compared to the viscous force in the matrix. This means the viscous force was not sufficiently high to displace a significant amount of oil from the pores. The biggest amount of oil production, in this case, would come mainly from the fractures. The remaining production came from gravity segregation (only in parts of the reservoir where capillary pressure is negligible) as it was discussed in chapter 2.2.2.1 "Gravity Drainage Assuming Homogeneous Vertical Saturation" and other displacement processes to a certain amount like fluid expansion due to pressure drop in the fractures related to hydrocarbon production. The gravity number in the fractures indicated that the gravity force was dominating

over the viscous force within the fractures, which implies that the fluid transport was only related to the density difference between oil and water. With the increase of capillary number, the oil recovery increased as well. The increase of capillary number during water flood could be related to the increase of viscous force. This means during the water injection the interfacial tension and viscosity of oil did not change significantly, which implies that the velocity has increased and was a result of pressure differential increase. Furthermore, gravity segregation as discussed before is another important displacement process and might have a significant effect to a certain point on capillary number increase due to an additional pressure differential at the interface of matrix block and fracture network as it can be seen in Figure 8. Another important displacement process will be capillary imbibition. If the reservoir is water wet, and the fractures are filled with water, spontaneous capillary imbibition would be applied to the matrix block until capillary pressure is zero. Due to the spontaneous imbibition a countercurrent flow occurs, which means the wetting phase in the fractures enters the matrix by expelling the oil from the pores. However, the capillary pressure is smaller than zero related to the capillary imbibition curve in oil-wet reservoirs. This means water will not enter the pores spontaneously. To overcome the problem, the capillary pressure must be changed. This can be done by surfactants and alkaline and will be discussed later. While the capillary number and oil recovery increased, the gravity number did not change significantly. It implies that the fluid transport occurs within the fractures only by density differences between the displacing fluid and displaced fluid and enforces the gravity segregation effect between fracture and matrix interface as displacement process for oil from the matrix into the fractures. In general, the pressure difference is insufficient to apply a significant viscous force in the fractures, which could be more dominant in the matrix system related to a smaller pore structure.

Regarding the ASP flood, the capillary number increases dramatically related to the reduction of interfacial tension by surfactants and alkaline. The chemicals are able to reduce a significant amount of residual oil. Generally, water wet reservoirs have higher residual oil saturations compared to oil wet reservoirs. If chemicals like alkaline and surfactants are used in water-wet reservoirs, there is a potential to reduce the residual oil saturation in the matrix significantly. However, if the reservoir is oil wet, there are intentions to change the wettability from oil to water wet by using alkaline and surfactant to mobilize oil, which is attached to the mineral surface. Another objective for wettability change is to enhance spontaneous imbibition of the aqueous phase. This will be done by shifting the capillary imbibition curve into the positive area of capillary pressure. Due to the change from oil wet to more water-wet condition, spontaneous imbibition is enhanced and the chemical displacing fluid is able to get soaked much deeper into the matrix blocks and improves the oil recovery. However, it should be noticed the wettability change from water to oil wet could be unfavorable because a significant

amount of oil could be trapped in the matrix system, which increases the residual oil saturation. If the wettability is changed in the fractures, the possibility of trapping in fractures compared to complex matrix pore geometry is reduced. The mobilized oil is easily able to flow in the fractures, where the permeable fractures act as a highway for fluid flow. The gravity number in the ASP flood stayed at a similar level compared to the water injection. The chemical flood did not really affect the gravity or viscous force. Only the density difference could be slightly increased due to the injection of alkaline, surfactants, and polymer in the aqueous phase. However, the effect on the density difference is not the same, compared to gas injection. Due to small changes for gravity number, this implies that gravity effect of the different fluids dominated the main fluid transport in the fractures again. In addition, the polymer injection could help to reduce the early breakthrough of the displacing fluid by blocking the high permeable fractures during the chemical flood and post water flush. Furthermore, it allows the surfactant and alkaline solution to imbibe deeper into the matrix block. One of the objectives of this thesis was to generate surface models for the complex relationship between fracture and matrix interaction during different displacement process. This mean, the calculated capillary number in the matrix and gravity number in the fracture network at a given position between injector and producer versus oil recovery rate should be plotted in 3D and allows easily determining the physical forces during the flooding process. This behavior can be seen in Figure 22 and Figure 23. The minimum and maximum values for each scenario were marked in the contour plot. Furthermore, it is possible to establish different capillary and gravity number the related recovery and forces during the flood. The shaded area in Figure 22 represents water injection; the remaining area represents the chemical flood.

4.2.5 Results of the effect of different parameters (Tornado plots)

The sensitivity analysis gives the possibility to figure out the influences of each varying parameter on the oil recovery. Due to the utilization of the benefits of RSM, a Tornado plot is able to represent these influences. Furthermore, the plot shows the positive or negative effects on the oil recovery factor. The Tornado plot contains linear, quadratic and interaction terms, which is related to the mathematics of the RSM approach. Regarding Figure 24 and Figure 25, the Tornado plot shows the most significant terms affecting the oil recovery factor related to the base case. Regarding the simulated experiments in water injection, the mean oil recovery factor is approximately 38%. As it can be seen from Figure 24, the most significant terms (i.e. main effects and interaction or cross terms) in the water injection case are the interaction terms and some linear and quadratic terms, which have a considerable effect on the recovery factor. Other effects of linear terms and cross terms have a moderate impact on the oil recovery factor.

The porosity had the biggest influence on the oil recovery factor as a linear term. However, it is interesting that the oil recovery decreased while the porosity increased. If the pore volume is small, the injection fluid volume is sufficient to displace a significant amount of oil in the pores, however if the pore volume exceeds the injection fluid volume significantly, the injection fluid volume could be insufficient to displace the same amount of oil compared to the case if the pore volume is very small. However, the quadratic effect of porosity had a considerable benefit for the oil recovery (+32.78%) as well. If the minimum value of the porosity range is squared, it results in a very low value ($Porosity^2 = 0.01^2 = 0.001$). If the maximum value of the porosity range is squared, it results in a lower value compared to the maximum single value of the porosity range ($Porosity^2 = 0.4^2 = 0.16 < 0.4$). Regarding to before mentioned linear effect of porosity, the oil recovery factor decreases with increasing porosity. If the values for porosity are squared, the resulting values are smaller compared to the single values of the range. Furthermore, it confirms the before mentioned porosity tendency and results in an increase in oil recovery to a certain point. However, if the porosity value is increased further, the quadratic response is increased as well, which results in a decrease in oil recovery in the end. In contrast, the quadratic effect of the vertical matrix permeability had a negative effect on the oil recovery factor. If the minimum value of the vertical permeability range is squared, it results in a very high value compared to the single permeability value ($Vertical\ Matrix\ Permeability^2 = 100^2 = 10000$). A vertical matrix permeability of 10000 and more has definitely a negative effect on the oil recovery. Generally, an increase of matrix permeability improves the oil recovery behavior anyway. However, if a certain value is reached, the benefit of higher matrix permeability decreases significantly. Anyway, only the interaction terms and linear terms are important for the interpretation of how they will influence the oil recovery factor. The quadratic terms are only important for the curvature of the related polynomial. The cross-term effects dominated the influence on oil recovery as well. The porosity, the vertical and horizontal permeability, and injection rate are included in the most important interaction terms. The cross term of two parameters implies that the effect of one parameter is more remarkable when the other parameter is moving to its extreme. Furthermore, it means the parameters interact with each other and have a combined effect on the result. As it can be seen from, the interaction term 'Vertical Matrix Permeability * Matrix Porosity' had some positive effect on the oil recovery factor. This means that the influence on the oil recovery to the 'Vertical Matrix Permeability' is high when the value of the 'Matrix Porosity' is high (+21.6% in oil recovery factor). A similar phenomenon occurred for the cross term 'Injection Rate * Matrix Porosity', however, the interaction term had a negative effect on the oil recovery factor (-9.726% in oil recovery factor). This means that the negative effect of increasing porosity is dominant over the positive effect by increasing the injection rate. Regarding to the ASP flood, the mean value for oil recovery

rate for ASP is approximately 61%. As can be seen from Figure 25, the most significant influences for oil recovery were linear, quadratic and cross terms for porosity and matrix permeability. Responses from injection rate, fracture permeability, and fracture spacing had moderate importance. The porosity had a similar impact on oil recovery factor for the ASP flood compared with the water flood. However, the matrix permeability had significantly more influence on the oil recovery compared to the water flood. A higher matrix permeability represents better access to the pore system, which allows the chemical displacing fluid to remove a significant amount of residual oil. The cross term 'Mat Perm J log * Frac Perm J' had a negative influence on oil recovery. The increase of fracture and matrix permeability in the same direction, reduce the possibility of the displacing fluid to imbibe into the matrix system. The displacing fluid will flow in the fracture than in the matrix regarding to the high fracture permeability. In contrast, the cross term 'InjRate ASP * Mat Perm J log' had a positive impact on oil recovery. The importance of the injection rate during the ASP flood is increased, while the horizontal matrix permeability moved to its extreme. Similar behavior occurred for all cross terms.

Chapter 5

Conclusion

5.1 Summary

The main idea of the thesis was to analyze, which physical forces were acting during water injection and chemical flood period. In the beginning, a reservoir model had to be set up by using a commercial reservoir simulator. For the establishment of the forces, several simulations (sensitivity analysis) for a given reservoir had to be done where the recovery factor, capillary, and gravity number were calculated. The capillary and gravity number should give a feeling, which physical forces were acting during the displacement process. The Experimental Design and RSM approach were used to generate a sufficient number of experiments. Afterward, the calculated data were analyzed by using a regression tool and for each case, an individual polynomial was generated. By utilization of the polynomials, three-dimensional plots could be produced to show the effects of gravity, capillary and viscous forces on hydrocarbon recovery in a naturally fractured reservoir. In addition, a Tornado plot was generated for each flooding scenario to analyze different impacts on the oil recovery factor based on the input parameters. Furthermore, saturation profiles were generated to show the flow of the displacing fluid through the naturally fractured reservoir.

5.2   Evaluation

One of the objectives was to analyze, which physical forces were acting during a water injection or injection of Alkaline-Surfactant-Polymer fluid in natural fractured reservoirs. To evaluate these forces, reservoir simulations were done and capillary and gravity numbers were calculated. By using these numbers, it was possible to evaluate possible displacement mechanisms like capillary, gravity or viscous dominated flow. The dimensionless numbers would be coupled with the oil recovery factor to show how the different forces affect the oil recovery. Another objective was to visualize the complex relationship during a displacement process like a chemical flood in a natural fractured reservoir. This would be done by using the evaluated polynomials for the response surface model and generating three-dimensional plots where recovery factor is a function of gravity and capillary number. By utilization of RSM, it was possible to generate a Tornado plot, which showed the impacts of each input parameter on the oil recovery factor. The different effects of the input parameters were analyzed and should give an overview, which parameters are the most sensitive ones.

5.3   Future Work

It has to be noticed that the reservoir model, which will be used in the thesis is a synthetic model. In reality, a natural fractured reservoir does not have uniformly distributed fractures. There are areas with low or high fracture densities. The reservoir matrix is not uniform as well. There are sweet spots and tight areas, where the reservoir permeability is locally very different from the average. For scientific research, the reservoir model was simplified by using uniform reservoir properties. In the end, results from a real reservoir could differ significantly from research studies. However, results from simplified models could give possible relationships during the displacement process, which could help to understand the complex processes in a real hydrocarbon reservoir. As it was mentioned before, the studies in this thesis and related papers only consider simplified synthetic reservoir models. For the application of chemical floods in a real reservoir, a lot of more effort is needed like injectivity tests, tracer tests, local reservoir chemistry. Information from these tests is additional input for the decision and implementation of chemical flooding in a naturally fractured reservoir.

Chapter 6

References

Abbasi Asl, Y., Pope, G. A. and Delshad, M. (2010) 'Mechanistic Modeling of Chemical Transport in Naturally Fractured Oil Reservoirs', *SPE Improved Oil Recovery Symposium*. Tulsa, Oklahoma, USA, 2010-04-24, Society of Petroleum Engineers.

Aguilera, R. (1987) 'Well Test Analysis of Naturally Fractured Reservoirs', *SPE Formation Evaluation*, pp. 239–252.

Aguilera, R. (1998) 'Geologic aspects of naturally fractured reservoirs', pp. 1667–1670.

Ahmed, T. H. (2010) *Reservoir Engineering Handbook*, 4th edn, Boston u.a., Gulf Professional Pub.

Akbar, M., Alghamdi, A. H., Herron, D. A. M., Olesen, Andrew Carnegie Dhruba Dutta Jean-Remy, Chourasiya, R. D., Stief, D. L. D., Netherwood, R., Russell, S.D. and Saxena, K. (2000) 'A Snapshot of Carbonate Reservoir Evaluation'.

Aziz, K. and Settari, A., eds. (1985) *Petroleum Reservoir Simulation*, London, Elsevier.

Babadagli, T. (2000) 'Scaling of Co-Current and Counter-Current Capillary Imbibition for Surfactant and Polymer Injection in Naturally Fractured Reservoirs', *SPE/AAPG Western Regional Meeting*. Long Beach, California, 2000-06-19, Society of Petroleum Engineers.

Bakhsi, P., Kharrat, R., Hashemi, A. and Zallaghi, M. (2017) 'Experimental evaluation of carbonated waterflooding: A practical process for enhanced oil recovery and geological CO_2 storage'.

Barenblatt, G. I., Zheltov, I.P. and Kochina, I. N. (1960) 'Basic Concepts in the Theory of Seepage of Homogeneous Liquids in Fissured Rocks'.

Blair, P. M. (1960) 'paper no. 1475G', *Trans. AIME secondary Rec. Symp*.

Bourbiaux, B. J. and Kalaydjian, F. J. (1990) 'Experimental Study of Cocurrent and Countercurrent Flows in Natural Porous Media', *SPE Reservoir Engineering*, vol. 5, no. 03, pp. 361–368.

Cheng, X., Kleppe, J. and Torsæter, O. (2018) 'Simulation Study of Surfactant Imbition Mechanisms in Naturally Fractured Reservoirs', *SPE Norway One Day Seminar.* Bergen, Norway, 2018-04-18, Society of Petroleum Engineers.

Da Silva, F. V. and Belery, P. (1989 - 1989) 'Molecular Diffusion in Naturally Fractured Reservoirs: A Decisive Recovery Mechanism', *Proceedings of SPE Annual Technical Conference and Exhibition,* 08.10.1989 - 11.10.1989, Society of Petroleum Engineers.

Delshad, M., Najafabadi, N. F., Anderson, G. A. and Pope, G. A. (2009) 'Modeling Wettability Alteration by Surfactants in Naturally Fractured Reservoirs'.

Dengen Zhou, F. J. Fayers, F. M. Orr Jr. (1993) 'Scaling of Multiphase Flow in Simple Heterogeneous Porous Media'.

Fadili, A., Kristensen, M. R. and Moreno, J. (2009) 'Smart Integrated Chemical EOR Simulation', *International Petroleum Technology Conference.* Doha, Qatar, 2009-12-07, International Petroleum Technology Conference.

Festoy, S. and van Golf-Racht, T. D. (1989) 'Gas Gravity Drainage in Fractured Reservoirs Through New Dual-Continuum Approach'.

Foulser, R.W.S. and Goodyear, S. G. (1989) 'Improved Stability of the IMPES Formulation for Chemical Flooding', *SPE Symposium on Reservoir Simulation.* Houston, Texas, 1989-02-06, Society of Petroleum Engineers.

Gilman, J. R. and Kazemi, H. (1988) 'Improved Calculations for Viscous and Gravity Displacement in Matrix Blocks in Dual-Porosity Simulators'.

Heeremans, J. C., Esmaiel, T. E. and van Kruijsdijk, C. P.J.W. (2006) 'Feasibility Study of WAG Injection in Naturally Fractured Reservoirs', *SPE/DOE Symposium on Improved Oil Recovery.* Tulsa, Oklahoma, USA, 2006-04-22, Society of Petroleum Engineers.

Heinemann, Z. E. and Mittermeir, G. (2014) 'Natural Fractured Reservoir Engineering'.

Jones, F. O. (1975) 'A Laboratory Study of the Effects of Confining Pressure on Fracture Flow and Storage Capacity in Carbonate Rocks', *Journal of Petroleum Technology*, vol. 27, no. 01, pp. 21–27.

Manrique, E. J., Muci, V. E. and Gurfinkel, M. E. (2007) 'EOR Field Experiences in Carbonate Reservoirs in the United States'.

Mohammed, M. N. and Hossain, M. E. (2016) 'A Numerical Investigation on the Performance of Alkaline-Surfactant-Polymer Flooding in Naturally Fractured Carbonate Reservoirs', *SPE Kingdom of Saudi Arabia Annual Technical Symposium and Exhibition.* Dammam, Saudi Arabia, 2016-04-25, Society of Petroleum Engineers.

Muskat, M., ed. (1946) *The Flow of Homogeneous Fluids Through Porous Media*, Edwards.

Muskat, M., ed. (1981) *Physical Principles of Oil Production*, 2nd edn, Boston, MA, International Human Resources Development Corporation.

Nelson, R. A. (1982) 'An Approach to Evaluating Fractured Reservoirs', *Journal of Petroleum Technology*, vol. 34, no. 09, pp. 2167–2170.

Ouenes, A. and Hartley, L. J. (2000) 'Integrated Fractured Reservoir Modeling Using Both Discrete and Continuum Approaches'.

Pirson, S. J., ed. (1958) *Oil Reservoir Engineering*, 2nd edn, New York (u.a), McGraw-Hill.

Quandalle, P. and Sabathier, J. C. (1989) 'Typical Features of a Multipurpose Reservoir Simulator', *SPE Reservoir Engineering*, vol. 4, no. 04, pp. 475–480.

Saad, N., Pope, G. A. and Sepehrnoori, K. (1989) 'Simulation of Big Muddy Surfactant Pilot'.

Sheng, J., ed. (2011) *Modern Chemical Enhanced Oil Recovery*, Gulf Professional Pub.

Shook, M., Li, D. and Lake, L. W. (1992) 'Scaling Immiscible Flow Through Permeable Media by Inspectional Analysis'.

Tang, G.-Q. and Firoozabadi, A. (2000) 'Effect of Viscous Forces and Initial Water Saturation on Water Injection in Water-Wet and Mixed-Wet Fractured Porous Media', *SPE/DOE Improved Oil Recovery Symposium.* Tulsa, Oklahoma, 2000-04-03, Society of Petroleum Engineers.

Treiber, L. E. and Owens, W. W. (1972) 'A Laboratory Evaluation of the Wettability of Fifty Oil-Producing Reservoirs', *Society of Petroleum Engineers Journal*, vol. 12, no. 06, pp. 531–540.

Uleberg, K. and Kleppe, J. (1996) 'Dual porosity, Dual Permeability Formulation for Fractured Reservoir Simulation'.

Warren, J. E. and Root, P. J. (1963) 'The Behavior of Naturally Fractured Reservoirs'.

Zellou, A. M., Hartley, L. J., Hoogerduijn-Strating, E. H., Al Dhahab, S.H.H., Boom, W. and Hadrami, F. (2003) 'Integrated Workflow Applied to the Characterization of a Carbonate Fractured Reservoir: Qarn Alam Field', *Middle East Oil Show.* Bahrain, 2003-06-09, Society of Petroleum Engineers.

Appendix A

Tables

Table 12 and Table 13 represents the coefficients of the response surface model for each depletion scenario. The coefficients are related to Equation 26 and were used to generate the surface planes. Table 14 and Table 15 represents the coefficients of the surface response for oil recovery. The coefficients are related to Equation 21 and were used to calculate the oil recovery factor for different sets of parameter values.

Table 12 – Surface Model Coefficients – Water Injection

Coefficient Type	Coefficient Value
P00	41.19
P10	1.518
P01	-1.959
P20	-0.25
P11	6.465
P02	-35.9059
X Average	1.246E-5
STD of X	5.959E-5
Y Average	41.02
STD of Y	4.485

Table 13 – Surface Model Coefficients – ASP

Coefficient Type	Coefficient Value
P00	80.21
P10	5.168
P01	-1.07
P20	-0.6543
P11	-0.4747
P02	-50.711
X Average	2.86E-3
STD of X	1.414E-2
Y Average	37.14
STD of Y	14.86

Table 14 – Coefficients of the Actual Parameters for Oil Recovery Function in ASP

Term	Coefficient
Intercept	60.4002
Frac_Spac_J	1.70711
Frac_Spac_K	-0.157995
InjRate_WF1	0.0655266
InjRate_AS	0.111903
Frac_Spac_I	2.98195
InjRate_ASP	0.152868
InjRate_SP	0.0356996
InjRate_WF2	0.0209047
Frac_Perm_I	-0.00207638
Mat_Perm_I_log	17.5228
Mat_Perm_J_log	6.35795
Frac_Perm_J	-0.00330213
Mat_Perm_K_log	3.18461
Por	-260.329
Frac_Spac_J*Frac_Spac_I	-0.24985
Frac_Spac_J*InjRate_WF2	-0.00740193
Frac_Spac_J*Mat_Perm_J_log	0.793263
Frac_Spac_K*Mat_Perm_I_log	-1.08847
InjRate_WF1*Frac_Spac_I	-0.0179673
InjRate_WF1*Mat_Perm_I_log	-0.0523084
InjRate_AS*InjRate_ASP	-0.000995417
Frac_Spac_I*Mat_Perm_J_log	0.666684
InjRate_ASP*Mat_Perm_J_log	0.0723204
Mat_Perm_I_log*Mat_Perm_I_log	5.69545
Mat_Perm_I_log*Mat_Perm_J_log	-7.61754
Mat_Perm_J_log*Mat_Perm_J_log	7.0906
Mat_Perm_J_log*Frac_Perm_J	-0.00976343
Frac_Perm_J*Mat_Perm_K_log	0.00408888
Mat_Perm_K_log*Mat_Perm_K_log	-2.99598
Mat_Perm_K_log*Por	16.7305
Por*Por	348.276

Table 15 – Coefficients of the Actual Parameters for Oil Recovery Function in Water Injection

Term	Coefficient
Intercept	46.3552
Frac_Spac_I	0.203365
Frac_Spac_J	2.93628
Inj_Rate	0.242884
Frac_Perm_I	-0.00114323
Mat_Perm_log_I	-2.46924
Mat_Perm_log_J	15.0423
Frac_Perm_J	-0.00230492
Mat_Perm_log_K	-7.25152
Frac_Perm_K	0.00568546
Por	-192.648
Frac_Spac_I*Inj_Rate	-0.0185754
Frac_Spac_I*Mat_Perm_log_I	0.654983
Frac_Spac_I*Frac_Perm_K	0.00222582
Frac_Spac_J*Frac_Spac_J	-0.480601
Frac_Spac_J*Mat_Perm_log_K	0.674284
Inj_Rate*Por	-0.498748
Frac_Perm_I*Mat_Perm_log_I	-0.00489838
Mat_Perm_log_I*Mat_Perm_log_J	-2.17748
Mat_Perm_log_I*Frac_Perm_J	0.0062892
Mat_Perm_log_J*Frac_Perm_J	-0.00551539
Mat_Perm_log_J*Mat_Perm_log_K	-2.50238
Mat_Perm_log_J*Frac_Perm_K	-0.00580347
Mat_Perm_log_J*Por	-16.7761
Frac_Perm_J*Mat_Perm_log_K	0.00637328
Mat_Perm_log_K*Mat_Perm_log_K	-4.70889
Mat_Perm_log_K*Por	42.5731
Frac_Perm_K*Por	-0.0459489
Por*Por	430.981

Equations

Equation 26 represents the polynomial, which was used for the three-dimensional representation. The coefficients can be seen in the before mentioned section and come from the Data Analysis Application in MATLAB. Equation 27 and Equation 28represents the normalization of each data point and is related to the regression tool.

$$Z = P00 + P10 * X + P01 * Y + P20 * X^2 + P11 * X * Y + P02 * Y^2 \qquad \text{Equation 26}$$

$$X_{norm} = \frac{X - \bar{X}}{STD} \qquad \text{Equation 27}$$

$$Y_{norm} = \frac{Y - \bar{Y}}{STD} \qquad \text{Equation 28}$$

MATLAB Code

```matlab
%% Calculation and Plotting of the Surface Models in
3D


% From the Curve Fitting Application in Matlab, a
polynom for each case
% will be evaluated. These polynoms were used to
generate calculated
% recovery factors (Z). Afterwards each data set (x,
y, Z) will be plotted
% as surface model.

x1=linspace(1e-5,1e-11,300);%Generating Nc_Matrix
values.
y1=linspace(0,70,300); %Generating Ng_fracture
values.

%% #1: Water Injection Case
p00=41.19;    %These values come from the Curve Fit
App in Matlab and define
p10=1.518;    %the coefficients of the polynom.
p01=-1.959;
p20=-.25;
p11=6.465;
p02=-35.9059;

x_norm_1=(x1-1.246e-5)/(5.959e-5);
y_norm_1=(y1-41.02)/4.485;
%The polynom can be only used if the the x and y
values are normalized
%These values come from the Matlab Curve Fitting App.

[X,Y]=meshgrid(x_norm_1,y_norm_1); %creacting a
meshgrid of datapoints
% related to the initial starting vectors (x,y) and
which are normalized.

Z_1=p00+p10.*X+p01.*Y+p20.*X.^2+p11.*X.*Y+p02.*Y.^2;
%General polynom given by Matlab Curve Fitting App.

figure(1) %Enables a window with the following plots
(Surface Models).
```

```matlab
hSurface1=surf(x1,y1,Z_1);
% Surface Function to produce a surface model based
on initial starting
%vectors and the calculated values from the polynom.
%
set(hSurface1,'FaceColor','yellow','EdgeColor','none'
);
% lFunction which colour the surface model yellow and
surpress meshgrid
% lines.

hold on %Enables to plot several models in one plot.


%% #2: ASP

x2=linspace(1e-1,1e-5,300);%Generating Nc_Matrix
values.
y2=linspace(0,70,300); %Generating Ng_fracture
values.

p00=80.21;
p10=5.168;
p01=1.07;
p20=-0.6543;
p11=-0.4747;
p02=-50.711;

x_norm_2=(x2-0.00286)/(0.01414);
y_norm_2=(y2-37.14)/14.86;
[X,Y]=meshgrid(x_norm_2,y_norm_2);
Z_2=p00+p10.*X+p01.*Y+p20.*X.^2+p11.*X.*Y+p02.*Y.^2;

hSurface2=surf(x2,y2,Z_2);
set(hSurface2,'FaceColor','blue','EdgeColor','none');

legend('Water Injection','ASP')
%Gives a legend with the before mentioned names.

hold off %Indicates to stop plotting follwing graphs
in one plot.
%
zlim([0 100]) %Limits the z axes.
xlim([1e-11 1e-1])
ylim([25 60])
set(gca,'XScale','log') %Change the x-axes to log
scale.
```

```matlab
set(gca,'FontSize',15) %Change the Font Size of the
plot.
view(68,44) %Rotate the 3D graph in specific
position.
grid on %Enables grid lines within the plot.
xlabel('Nc Matrix') %Indicate the name of x-axes.
ylabel('Ng Fracture') %Indicate the name of y-axes.
zlabel('Recovery Factor [%]') %Indicate the name of
z-axes.

%% Generates again Surface Models, however it will be
used for 2D View
% A third window will be openend with different grid
visualizations.
% The 3D will be rotated in 2D position (Nc vs. Ng
and Recovery Factor as
% colourbar).

figure(2) %Second plot will be openend.

hold on

hSurface3=surf(x1,y1,Z_1);
set(hSurface3,'LineStyle',':') %LineStyle function
% generates meshgrid with
% with different types of lines.

hSurface4=surf(x2,y2,Z_2);
set(hSurface4,'LineStyle','none');
hold off

d=colorbar;
caxis([0 100])
xlim([1e-11 1e-2])
d.Label.String='Recovery Factor [%]';
xlabel('Nc Matrix')
ylabel('Ng Fracture')
legend('Waterflood','ASP')
set(gca,'XScale','log')
set(gca,'FontSize',15)

view(0,90)
```